

UCSF

UC San Francisco Electronic Theses and Dissertations

Title

The role of autism genes in enteric neuron development and function

Permalink

<https://escholarship.org/uc/item/0p2856sm>

Author

McCluskey, Kate

Publication Date

2024

Peer reviewed|Thesis/dissertation

The role of autism genes in enteric neuron development and function

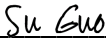
by
Kate Elizabeth McCluskey

DISSERTATION
Submitted in partial satisfaction of the requirements for degree of
DOCTOR OF PHILOSOPHY

in
Neuroscience


in the
GRADUATE DIVISION
of the
UNIVERSITY OF CALIFORNIA, SAN FRANCISCO

Approved:

DocuSigned by:
 Su Guo
607F1205C317481... Chair

DocuSigned by:
 Helen Willsey

DocuSigned by:
 Erica J Hutchins

DocuSigned by:
 DEVANAND MANOLI
0C4570A6FDE94F2...

Committee Members

Copyright 2024

by

Kate Elizabeth McCluskey

Acknowledgements

Dearest to me, I would like to thank my family. To my parents Pam and Kevin and my brother Chris, thank you for the immense support and encouragement you have always given me. You have gotten me through the toughest parts of this journey and have celebrated everything with me along the way. I could not have done this without you and I am so grateful for your love.

To my mentor Helen, thank you for going on this journey with me. I don't think either of us knew what we were getting into when I asked to learn how to work with the frogs. Thank you for your incredible mentorship – I feel very lucky to have been a part of your lab. You have taught me so much about being a scientist and mentor; to fully embrace a challenge and the importance of having fun doing what you love. I hope that if I am fortunate enough to have my own lab someday that I can cultivate an environment of curiosity, comradery, and scientific excitement as you have done.

To Charlotte, Hasan, and Elina, thank you for being my best friends through this process. You have all brought light and laughs to this experience. And to the current froggers, thank you for creating such a wonderful place to do science everyday. Also to Cameron Exner, thank you for being you. You always put your entire self into your teaching and mentorship – anyone that is able to cross paths with you is lucky. I am immensely grateful to have you as a mentor and friend.

I would also like to thank the entire *Xenopus* community for being such an incredible source of support and encouragement. Specifically, Lance Davidson and Chenbei Chang for inspiring me to take time in the lab to play.

I would also like to thank the Neuroscience Program, especially our administrators Pat Veitch and Lucita Nacionales for their work in taking care of all of us. And of course, thank you to my thesis committee members Su Guo, Dev Manoli, and Erica Hutchins for their invaluable input on this project and their life advice.

And to my partner Sam, thank you for relating to all the PhD memes with me. Thank you for moving across the country with me and for your everyday support. No matter the day I had in lab, it is always a joy and comfort to come home to you. Thank you for prioritizing fun and helping me have a healthy work/life balance. I have loved equally all our adventures and lazy weekends together. I'm grateful for our time together in California and look forward to our next chapter.

Contributions

Chapter 1 was written by Kate E McCluskey

Chapter 2 was written by Kate E McCluskey and contains unpublished findings with contributions from Kate E McCluskey, Katherine M Stovell, Liliya von Behren, and Helen R Willsey.

Chapter 3 was reproduced in its entirety from:

McCluskey, KE, Stovell, KM, Law, K, Kostyanovskaya, E, Schmidt, J, Exner, CRT, Dea, J, Brimble, E, State, MW, Willsey, AJ, Willsey, HR, “Autism gene variants disrupt enteric neuron migration and cause gastrointestinal dysmotility” (*bioRxiv*).

The role of autism genes in enteric neuron development and function

Kate Elizabeth McCluskey

Abstract

Food consumption is one of our basic needs, yet many people experience gastrointestinal distress with almost two-thirds of Americans self-reporting symptoms. The prevalence of clinical gastrointestinal diagnoses is higher in populations with developmental disorders such as Autism, developmental delay, and Down Syndrome. These issues are often a result of gut dysmotility, which can present as constipation, diarrhea, esophageal reflux, etc, symptoms that are also significantly associated with poorer quality of life in affected individuals. Even with these high prevalence rates and impact on quality of life, the underlying biology of gastrointestinal issues is poorly understood.

The gastrointestinal tract is completely innervated and controlled by the enteric nervous system. The development of the enteric nervous system has been characterized in classic models such as chicks, mice, and zebrafish, however, little is known about how the development of the enteric nervous system may be disrupted in developmental disorders such as autism. This dissertation focuses on the question of why gastrointestinal issues are comorbid with neurodevelopmental disorders. In chapter 2, we establish *Xenopus* as a new model to study the development and function of the enteric nervous system. In chapter 3, we use this model and find that high-confidence autism variants are required for enteric neuron migration and gastrointestinal motility.

Table of Contents

CHAPTER 1 Introduction.....	1
The enteric nervous system	1
Disorders of the enteric nervous system	2
Gastrointestinal issues in autism spectrum disorder	3
Serotonin as a key component in ENS development and function	6
Models to study the enteric nervous system	8
<i>Xenopus</i> as a model to study enteric neuron development	9
CHAPTER 2 Using the frog model <i>Xenopus</i> to study enteric nervous system development.....	12
Introduction.....	12
Results.....	13
Characterization of ENS precursors in <i>Xenopus</i>	13
Assessment of enteric neurons in <i>Xenopus</i>	15
<i>Xenopus</i> as a model to study Hirschsprung’s Disease	16
Novel assay to study gut motility in <i>Xenopus</i>	18
Discussion	20
Materials and Methods	29
CHAPTER 3 Autism gene variants disrupt enteric neuron migration and cause gastrointestinal dysmotility	33
Introduction.....	33

Results.....	35
hcASD gene expression is enriched in enteric neurons and their progenitors ...	35
Prevalence of GI dysmotility among patients with hcASD gene variants.....	35
hcASD gene variants disrupt ENS migration <i>in vivo</i>	36
Depletion of <i>dyrk1a</i> disrupts neural crest development and ENCC migration	37
Depletion of <i>dyrk1a</i> decreases gut motility <i>in vivo</i>	39
Serotonin reuptake inhibitor treatment rescues gut dysmotility following	
Dyrk1a inhibition	40
Discussion	41
Materials and Methods	62
References	70

List of Figures

CHAPTER 2

Figure 2.1. <i>phox2b</i> reliably marks enteric neuron progenitor cells in <i>Xenopus</i>	23
Figure 2.2. Enteric neuron organization is similar between <i>Xenopus</i> and humans	24
Figure 2.3. Hirschsprung's Disease risk gene <i>ret</i> is required for ENCC migration in <i>Xenopus</i>	25
Figure 2.4. Gut motility screen in <i>Xenopus</i> identifies modulators of gastric motility	27

CHAPTER 3

Figure 3.1. hcASD gene expression enrichment in human prenatal gut transcriptomic dataset.....	44
Figure 3.2. hcASD gene expression is enriched in ENS cells and individuals with pathogenic variants in these genes experience GI issues.....	45
Figure 3.3. hcASD gene expression in human prenatal gut transcriptomic dataset	46
Figure 3.4. hcASD gene depletion <i>in vivo</i> causes ENCC migration defects.....	47
Figure 3.5. Additional representative images of hcASD gene knockdowns	48
Figure 3.6. <i>dyrk1a</i> is expressed in ENCCs and Dyrk1a localizes to microtubule-based structures	49
Figure 3.7. hcASD gene <i>dyrk1a</i> perturbation reduces ENCC migration and decreases gut motility <i>in vivo</i>	50
Figure 3.8. <i>dyrk1a</i> is independently required for early neural crest development and for later ENCC migration.....	52

Figure 3.9. hcASD genes *chd8* and *chd2* are required for neural crest development... 54

Figure 3.10. Dyrk1a-associated gut dysmotility is ameliorated by acute exposure to
an SSRI or 5-HTR6 agonist 55

List of Tables

CHAPTER 2

Table 2.1. Gut motility drug screen results	28
---	----

CHAPTER 3

Table 3.1. Summary table of patient GI symptoms from Ciitizen® records for individuals with variants in <i>SYNGAP1</i>	57
--	----

Table 3.2. Summary table of patient GI symptoms from Ciitizen® records for individuals with variants in <i>SCN2A</i>	58
--	----

Table 3.3. Summary table of patient GI symptoms from Ciitizen® records for individuals with variants in <i>CHD2</i>	59
---	----

Table 3.4. Summary table of patient GI symptoms from Ciitizen® records for individuals with variants in <i>STXBP1</i>	60
---	----

Table 3.5. Summary table of patient GI symptoms from Ciitizen® records for individuals with variants in <i>SLC6A1</i>	61
---	----

List of Abbreviations

GI	Gastrointestinal
ENS	Enteric nervous system
CNS	Central nervous system
ENCC	Enteric neural crest-derived cell
HSCR	Hirschsprung's Disease
GERD	Gastroesophageal reflux disease
ASD	Autism spectrum disorders
ENCC	Enteric neural crest-derived cell
iPSC	Induced pluripotent stem cell
TPH	Tryptophan hydroxylase
SSRI	Selective serotonin reuptake inhibitor
5-HTR6	Serotonin receptor 6

CHAPTER 1

Introduction

The enteric nervous system

The enteric nervous system (ENS) is often referred to as the 'second brain' due to its complexity although, evolutionarily, it is considered the first brain¹. The ENS is the largest and most complex part of the peripheral nervous system and is unique in its morphology and circuitry². It consists of two subdivisions, the myenteric plexus and the submucosal plexus, which together control gastric motility, nutrient absorption, fluid secretion, and blood flow³. Although it is fully capable of operating independently from the central nervous system, the ENS communicates with the brain through the vagus nerve and is also interconnected with the spinal cord, immune system, enteroendocrine system, and microbiome⁴.

The development of the enteric nervous system is similar to that of the central nervous system (CNS) as both progress through neural progenitor proliferation, migration, differentiation and circuit formation³. In contrast to the CNS which develops from the neural tube, the ENS is completely derived from the neural crest – a majority originates from the vagal neural crest with small contributions from the trunk and sacral regions⁵. Neural crest cells are a highly migratory cell population, delaminating from the neural tube during early embryogenesis and traveling throughout the embryo to contribute to craniofacial cartilage, smooth muscle, pigment cells, and the peripheral nervous system⁶. Cells that migrate toward the foregut respond to local retinoic acid produced by the paraxial mesoderm and activate expression of the receptor tyrosine kinase, RET⁷.

This Ret-positive cell population, termed enteric neural crest-derived cells (ENCCs), begins to expand and colonize the gut. Their colonization depends on a highly proliferative wavefront of cells that advances throughout the entire gastrointestinal tract³. These cells form chains along the rostrocaudal axis which allow them to migrate more quickly and in a persistent direction⁸.

Once these ENCCs have reached their final destination, they differentiate into various subtypes of enteric neurons and glia as defined in part by their neurochemical coding⁵. The ENS uses the same neurotransmitters for neural communication as the brain, which can be used to identify different neuronal subtypes⁹. Studies in mice have shown that the first neurons to differentiate are cholinergic cells at E8 and E10.5, followed by serotonergic neurons at E11.5, dopaminergic and nitric oxide synthase 1-positive neurons at E15.5, and calretinin neurons around the time of birth⁴. Combinations of these neurons connect to form functional circuitry to control gastric motility^{10,11}. Inhibitory and excitatory motor neurons control the contraction and relaxation of gut muscle to coordinate moving contents through the gut^{10,11}. Motor neurons also communicate with sensory neurons closer to the lumen of the gut, which detect and respond to nutrients passing through^{10,11}.

Disorders of the enteric nervous system

However, these developmental processes can go awry and lead to dysfunction in the enteric nervous system. One of the most common disorders of the ENS is Hirschsprung's Disease (HSCR), a genetic disorder that affects roughly 1 in 5000 live births and results in hindgut aganglionosis, often caused by incomplete colonization of

the colon by enteric neurons^{12,13}. This absence of enteric neurons can also be due to disrupted cell proliferation, survival, or differentiation¹³. The current treatment for HSCR is surgical resection of the aganglionic portion of the gut, without which this condition is fatal¹³. Risk genes for HSCR include *SOX10*, *PHOX2B*, *RET*, and *EDNRB* which are required for the development of the neural crest and ENCCs⁵.

Achalasia, a motor disorder of the esophagus, is another common symptom associated with enteric nervous system dysfunction¹⁴. The loss of inhibitory neurons in the esophagus and lower esophageal sphincter result in dysregulated peristalsis¹⁵. Individuals suffering from achalasia regularly experience dysphasia and regurgitation of food, often leading to their misdiagnosis of gastroesophageal reflux disease (GERD)¹⁶. Achalasia is an incurable disease, yet palliative treatments involve botox, myotomy, or pneumatic dilation to relax the esophagus¹⁷. Although the causes of achalasia are unknown, abnormalities in immune-related genes have been associated with susceptibility to the disorder, specifically the human leukocyte antigen class II gene¹⁸.

Gastrointestinal issues in autism spectrum disorder

One population that experiences high rates of GI distress are individuals with autism¹⁹⁻²¹. Autism spectrum disorders (ASD) are heterogeneous neurodevelopmental conditions that are defined by social, behavioral, and communication difficulties²². This connection between ASD and gastrointestinal issues was first noted in 1943 by a physician describing children with ASD as having 'eating problems'²³. This highlights the difficulty in diagnosing gastrointestinal distress – it often relies on the individual communicating their problems to their healthcare provider. In the case of ASD

specifically, this can go unreported and untreated as individuals often have difficulties in communication²⁴. A meta-analysis of research on GI symptoms and ASD found that affected individuals experience GI distress 3-4 times more frequently than their neurotypical peers¹⁹. These issues also correlate with increased irritability and social withdrawal, highlighting the negative impact on their quality of life²⁵. Despite this well-established comorbidity, the underlying molecular mechanisms remain unknown.

There are a few major hypotheses in the field for why individuals with autism may be experiencing GI distress. First is the effect on the microbiome – studies have shown a dysregulation in the microbiota composition in GI tracts of individuals with autism^{26–28}. Although bacterial overgrowth has been observed in populations of affected individuals, no consistent change in composition has been noted across individuals. This suggests that changes in the gut microbiome may be a secondary effect of other dysfunction in the gut. For example, patients with Hirschsprung's Disease, which specifically affects the development of the enteric nervous system, often exhibit altered gut microbiome compositions likely as a result of reduced intestinal motility²⁹. A related idea focuses on the concept of a 'leaky gut' in individuals with ASD – that the intestinal epithelial barrier is compromised and allows bacteria and food components into the gut wall⁴. Although a popular hypothesis, there is limited evidence of abnormal GI permeability in individuals with ASD²¹.

Another avenue has explored the cell-intrinsic effects of autism-associated genetic variants. Over the past decade there has been a continued effort to identify genes that are highly associated with ASD^{30–32}. These studies have leveraged exome sequencing of thousands of family trios to identify large-effect, rare *de novo* variants. Unlike

common variants identified through GWAS studies, these *de novo* variants greatly increase the likelihood of a diagnosis of ASD³³. They are all heterozygous loss-of-function mutations, thus losing one copy of one of these genes is sufficient to greatly increase the likelihood of a diagnosis of ASD³³. To date, 252 genes have been identified as high-confidence ASD (hcASD) genes with an FDR of < 0.1³¹.

Work over the past 15 years has examined the effects of knocking down some of these top hcASD genes on the enteric nervous system. A mouse model of a conditional *PTEN* knockout in the ENS and pigment cells showed an increase in the number of enteric neurons along the gastrointestinal tract as well as evidence of intestinal pseudoobstruction³⁴. Their results mirror the chronic intestinal pseudoobstruction seen during pediatric consultations which can lead to mortality in patients. In 2014, Bernier et al. described the gastrointestinal complaints often experienced by many individuals with variants in the autism-associated gene *CHD8*³⁵. Of the 15 individuals included in the study, 12 reported significant GI distress, mainly constipation. Using the zebrafish model, they found that knockdown of *chd8* led to reduced gut motility in the animals as well as a reduction in the number of enteric neurons in the gut³⁵. Shortly after, a study described individuals with Pitt-Hopkins Syndrome as suffering from high rates of gastroesophageal reflux and constipation³⁶. They used a mouse model of Pitt-Hopkins Syndrome, caused by haploinsufficiency of *TCF4*, and observed reduced gut transit velocities while reporting no differences in gross gut anatomy³⁶. Specifically, they found that *Tcf4*^{-/-} mice have slowed gastric emptying and reduced propulsion in the distal part of the colon, similar to those symptoms described by affected individuals³⁶. Two more studies were published in 2019 examining *shank3a;shank3b* and *Foxp1*^{+/-} mutant

models. The first used zebrafish to model Phelan-McDermid Syndrome caused by haploinsufficiency of *SHANK3* in humans³⁷. Leveraging this mutant line, they found that these animals displayed decreased peristaltic frequency and slow GI transit³⁷. Although they did not observe statistical differences in the number of enteric neurons, they found a reduction in the number of enteroendocrine cells in the mutants compared to wildtype animals³⁷. The second study used a heterozygous *Foxp1* knockout mouse and observed impaired gastric motility and partial retrograde contractions, suggesting this may be due to dysfunction in the enteric nervous system³⁸. Although all of these studies have examined gastric motility and gut morphology, none of them have studied the development of the enteric nervous system itself. Autism is a neurodevelopmental disorder and this evidence suggests that perturbations in autism-associated genes may affect ENS development.

Serotonin as a key component in ENS development and function

Serotonin plays an important role in both the development and function of the enteric nervous system. Almost all of the body's serotonin is produced in the gut where two isoforms of the enzyme tryptophan hydroxylase (TPH) are responsible for this process³⁹. The first isoform, TPH1, is found in enterochromaffin and mast cells and the second, TPH2, is expressed in enteric neurons⁴⁰. Although enterochromaffin and mast cells produce the majority of intestinal serotonin, research has demonstrated that ENS development and function relies on that produced in neurons⁴⁰. Work using TPH2 knockout mice shows that these animals contain fewer enteric neurons overall as well as a disproportional decrease in later-born dopaminergic and GABAergic neurons,

demonstrating that these classes are more susceptible to the loss of serotonergic neurons⁴⁰. These mice also exhibit slowed gastric motility while TPH1 knockout mice do not differ from wildtype in enteric neuron number or gut transit time⁴⁰. While neuronal serotonin production is required for proper development, so is its action outside of the cell. Researchers found that a gain-of-function mouse model of the serotonin transporter, which increases the clearance of serotonin from the synapse, contains fewer numbers of enteric neurons and exhibits slowed gastrointestinal motility that could both be rescued by treatment with 5-HT receptor 4 agonist prucalopride when administered during development⁴¹.

Serotonin has also previously been associated with autism and GI distress^{37,39,41}. Increased blood serotonin levels, termed hyperserotomia, has been described in roughly 25% of individuals with autism and correlates with symptoms in the lower gastrointestinal tract⁴². Hyperactive variants of the gene that encodes for the serotonin transporter, *SLC6A4*, have been found in individuals with ASD⁴¹ and the *SHANK3* study described above found that knocking down expression of *shank3a;shank3b* led to a reduction in serotonin-expressing enteroendocrine cells which are responsible for producing much of the body's serotonin³⁷. Further, serotonin signaling is well-known for its role in gastrointestinal motility and as a result serotonergic drugs have been used in the management of functional GI disorders⁴³. Selective serotonin reuptake inhibitors (SSRIs) have been successfully used to ameliorate GI distress in cases of irritable bowel syndrome by increasing gut transit time⁴⁴. Due to this evidence, serotonin modulation may be a fruitful avenue in treating autism-associated GI distress.

Models to study the enteric nervous system

Early work performed in avians was essential in demonstrating that the enteric nervous system is derived from the neural crest through both ablation⁴⁵ and chick-quail graft studies⁴⁶. The chick model offers a myriad of useful methods to study neural crest migration⁴⁷ that have been leveraged to perform lineage tracing studies and offer insights into regional contributions of the vagal neural crest to sections of the enteric nervous system⁴⁸. As demonstrated above, rodents and zebrafish are also popular models for studying the gut and ENS. Each of these models have established methods for examining gut transit as well as available mutant animal lines⁴⁹⁻⁵². The mouse gastrointestinal tract consists of the duodenum, jejunum, ileum, cecum, and proximal and distal colon, similar to that of humans⁵³. The architecture of the ENS is also complex in mice, with regional differences in neuronal subtype composition and shares a similar transcriptional program to the enteric nervous system in humans⁹. However, the mouse is a low through-put model and requires *ex vivo*⁵⁴ or cell culture⁵⁵ experiments to study enteric neuron activity. In contrast, the zebrafish model provides the ability to study gut motility and peristalsis *in vivo* due to their inherent transparent appearance³⁷. With the use of available transgenic lines, enteric neuron progenitors (ENCCs) can be imaged live during development to observe their migration⁵². Additionally, high-throughput experiments are often performed in zebrafish as they produce a large number of offspring during matings and are easily injected to knockdown gene expression with the use of morpholinos⁵⁶. A few drawbacks of this model are the inherent simplicity of the zebrafish gut, since it is a tube-like structure that

lacks a stomach⁵⁷, as well as its tetraploid genome⁵⁸ which makes the use of CRISPR/Cas9 a technical challenge.

One other emerging model is induced pluripotent stem cell (iPSC)-derived enteric neurons and ENCCs⁵⁹. In the past few years protocols have been established to derive iPSCs into enteric neurons⁶⁰ or enteric neuron progenitors⁶¹. These methods are useful in specifying and enriching for certain types of cells and CRISPRa/i can be used to activate or repress genes, respectively⁶². However, a major drawback of monolayer iPSC-derived cell culture is their inability to recapitulate *in vivo* cell behavior⁶³. Altogether this highlights the need for a model in which genes can easily be knocked down with CRISPR and studied *in vivo* in a high throughput manner.

***Xenopus* as a model to study enteric neuron development**

The frog model *Xenopus* is poised to fill this need as a model to study ENS development and function *in vivo*. Two species of *Xenopus* are commonly used in biomedical research: *Xenopus laevis* and *Xenopus tropicalis*. *X. laevis* have much larger embryos that are hardier and easier to use for assays involving explants and live imaging^{64,65}. *X. tropicalis* have a diploid genome that is highly conserved compared to humans⁶⁶ and, compared to the pseudo-tetraploid genome of *X. laevis*, are easier to use with the CRISPR/Cas9 system to create genetic knockdowns⁶⁷. Many benefits of *Xenopus* as a model are shared by both species, such as the ease of using pharmacological inhibitors by adding them to media and the production of thousands of embryos per mating⁶⁸. One of the most unique aspects of *Xenopus* is their well-characterized fate map^{69,70}. Individual blastomeres at the 32-cell stage can be

injected with morpholinos, CRISPR, or mRNAs to target specific cell lineages in the embryo. One common and powerful way to leverage this attribute is by performing unilateral injections into one cell at the 2-cell stage, since each of these cells will develop into the left or right side of the animal, and comparing against the contralateral in-animal control side⁷¹⁻⁷³. Due to these advantages, *Xenopus* has emerged as a powerful model to study human genetic disorders⁷⁴.

The tadpole gut has previously been described and established as a useful model to investigate digestive organ development⁷⁵. Compared to zebrafish which have a simpler gut morphology, the *Xenopus* tadpole gut has separate foregut, midgut, and hindgut regions and stereotypical coiled morphology that begins forming in the late tailbud stage⁷⁶. The ENS was initially described in *Xenopus* in 1990 by differential staining with the *X. laevis* - *X. borealis* nuclear marker system to show that neural crest cells colonize the gut and differentiate into enteric ganglia⁷⁷. As a result, subsequent studies focused on determining the subtypes of enteric neurons in the *Xenopus* gut. Co-staining with Acetylated Tubulin to mark enteric neurons, the frog gut has been shown to contain GABA, NOS, PACAP, and VIP neurotransmitters beginning at NF st41⁷⁸ and additionally 5-HT during metamorphosis⁷⁹. The *Xenopus* model has the capacity to study gut development and the enteric nervous system as well as model genetic developmental disorders in a high-throughput way.

This dissertation aims to develop *Xenopus* as a model and begins to address the question of how ENS development may be perturbed in the context of neurodevelopmental disorders. In **Chapter 2**, we provide evidence to support *Xenopus* as a model for ENS development by establishing reliable markers and developmental

timepoints to visualize enteric progenitor cells. We also develop novel assays to measure the effect of genetic and pharmacological perturbations on ENS development and, as a proof of principle, model Hirschsprung's Disease. We further expand this model to study gut motility in a novel, high throughput assay. In **Chapter 3**, we apply these established methods to study gastrointestinal distress in autism. We show that top high-confidence autism genes are required for enteric neuron migration and function.

CHAPTER 2

Using the frog model *Xenopus* to study enteric nervous system development

Introduction

The enteric nervous system (ENS) is an intricate portion of the peripheral nervous system that controls gut motility as well as nutrient absorption, fluid secretion, and blood flow³. The enteric nervous system was first described in the frog model *Xenopus* in 1990 when researchers demonstrated that it is derived from the neural crest, similar to what had previously been shown in avians⁷⁷. This sparked interest in describing the development of the ENS in *Xenopus* and its similarities to human development. As a result, followup studies investigated the presence of various neurotransmitters (VIP, PACAP, NOS, tachykinins SP/NKA, and CGRP) by immunofluorescence staining to visualize enteric neuron subtypes⁷⁸. These neurotransmitters appear in the same order developmentally as those in the human GI tract⁷⁸ and are required for proper gut motility^{80,81}. Human fetal gut motility begins in the third trimester as an uncoordinated pattern which develops into migrating motor complexes⁸². Similar development has been observed in *Xenopus*, with spontaneous gut motility beginning at NF stage 41 that matures into coordinated wave patterns organized by enteric neuron activity and coincides with exogenous feeding at NF stage 47⁸². These established similarities between *Xenopus* and human ENS position the frog to serve as an excellent model to study these processes in development and disease.

Here we describe *Xenopus* as a model to assess the development and function of the enteric nervous system. We demonstrate that the marker gene *phox2b* can be used reliably to visualize enteric neural crest-derived cells (ENCCs) which migrate through the early gut mesenchyme at NF stages 39-41. Later in development, we identify mature enteric neurons through co-staining for the pan-neuronal marker HuC/D and Acetylated α -Tubulin. To test this model, we focus on the Hirschsprung's Disease risk gene *ret* to show that it is required for ENCC migration as shown in early and late stage ENS visualization. Finally, we develop a novel gut motility assay and identify small molecule modulators of gut transit time. These results demonstrate how *Xenopus* can be used to investigate the development of enteric neurons and their function in the context of disease.

Results

Characterization of ENS precursors in *Xenopus*

We first set out to identify a reliable way to visualize the developing enteric neurons in tadpoles and optimal timepoints for assaying these cells. The ENS is derived from the neural crest and as a result early neural crest cells and later ENCCs express *sox10* as they migrate². Once these neural crest cells specify into ENCCs, they begin to additionally express *phox2b*². These two marker genes remain expressed until ENCCs differentiate into neurons or glia and retain only *phox2b* or *sox10* expression respectively². Common models such as mice⁸³ and zebrafish⁸⁴ use *phox2b* to visualize these cells. *phox2b* has previously been stained in *Xenopus*, but only assessed in neurula stage embryos and the head region and pharyngeal arches at NF stage 35⁸⁵.

According to single-cell sequencing data in *Xenopus*⁸⁶, the *phox2b* expression slope increases at NF stage 31 and peaks at NF stage 40 (**Fig 2.1A**, adapted from Xenbase⁸⁷). This increase is similar to the *sox10* transcript slopes at these same stages suggesting that these are the timepoints when ENCCs are specifying and migrating through the gut. Therefore, we decided to assess both *phox2b* and *sox10* over early development to determine if these genes could serve as markers for ENCCs.

At early neurula stages before the vagal neural crest begins migrating, *phox2b* marks the hindbrain region⁸⁸. The areas positive for *phox2b* are part of the neural tube, medial to the *sox10* positive areas of the neural crest at stages 15 and 20 (**Fig 2.1B**). Eventually the vagal neural crest cells migrate into the gut and become ENCCs which we can visualize at NF stage 40 as puncta in the gut region with both *sox10* and *phox2b* probes. From the *sox10* staining at stage 40, we observe striations near the neural tube that are likely streams of cells migrating into the gut between the somites. Once these cells enter into the gut region, they begin expressing *phox2b* (**Fig 2.1B**). Moving forward, we chose to use *phox2b* as a marker for ENCCs at later stages since the staining is much clearer than *sox10* and is more specific to these cells.

To assess how these ENCCs develop over a range of developmental timepoints, we stained for *phox2b* in wildtype embryos at NF stages 39, 40, and 41 (**Fig 2.1C**). We observed that these cells migrate through the gut first invading the anterior end and later colonizing the posterior region, consistent with the anterior-posterior migration described previously⁷⁷. At stage 39 these cells occupy about 30% of the gut, by stage 40 roughly 70% of the gut is occupied, and by stage 41 these cells cover almost the entire side of the gut. We decided to conduct experiments at stage 40 since this would

allow us to observe both increased or decreased changes in migration area as a result of developmental perturbations.

Assessment of enteric neurons in *Xenopus*

To investigate mature enteric neurons, we used immunofluorescence staining with antibodies against Acetylated α -Tubulin as it has been previously used to mark neuronal projections^{77,78} along with the pan-neuronal protein HuC/D⁸⁹ and phalloidin to stain the F-actin in muscle cells and demarcate the entire gut (**Fig 2.2A**). We stained across developmental time, from NF stage 42 to NF stage 45 and observed that the organization of enteric neurons and their projections becomes more structured over development, eventually forming parallel tracks that follow the curvature of the gut (**Fig 2.2B**). In contrast to the adult gut which contains enteric ganglia, these early stage neuronal bodies are generally spaced out from each other which is similar to mammalian fetal ENS architecture⁵³.

While staining for Acetylated α -Tubulin, we also noticed unique circles of tubulin in the gut at each of these timepoints. At NF stage 45, we observed groups of circles within the gut and that these circles often localize near enteric neuron projections (**Fig 2.2C**). Further staining for DAPI shows that these circles are nucleated cells that are not currently dividing. We hypothesize that these cells may be ENCCs capable of differentiating into enteric neurons.

We also sought to assess the distribution of neuronal subtypes in the *Xenopus* gut at stage 46 (**Fig 2.2D**). We used antibodies against Calretinin, 5-HT, neuronal NOS, and Tyrosine Hydroxylase and co-stained for Acetylated α -Tubulin. We found that there are

a small number of Calretinin+ neurons as well as some 5-HT+ cells in the gut. From this staining it is unclear whether 5-HT is co-localizing with neuronal bodies. We also observed a large number of nNOS+ neurons, which is a major inhibitory cell population in the ENS⁹⁰. We did not observe any Tyrosine Hydroxylase staining in the gut, although we did observe a positive population in the brain (data not shown) suggesting that there is no production of catecholamines in the gut at this time.

***Xenopus* as a model to study Hirschsprung's Disease**

To assess the effects of perturbations on the system we took two parallel approaches: a genetic or a timed pharmacological knockdown which each leverage one of the strengths of the *Xenopus* model (**Fig 2.3A**). First, we used a unilateral injection of a morpholino to knockdown the expression of a gene of interest on one side of the animal allowing us to compare the area of ENCC migration between the injected and contralateral uninjected control sides. These comparisons within an animal reveal subtle differences that may be missed when only comparing between individuals⁷¹. The second approach pharmacologically inhibits a protein of interest without affecting early events such as gastrulation and neurulation. This small molecule treatment only inhibits the protein after the neural crest has specified and begins migrating. Therefore, we can avoid any effects that the genetic knockdown may have on early embryogenesis and more specifically observe the effects on neural crest migration.

Since Hirschsprung's Disease (HSCR) affects the development of the enteric nervous system and results in reduced colonization of the gut by enteric neuron progenitors, we decided to test our model by targeting genes and proteins associated with the disorder.

First, we created a morpholino to genetically knockdown *ret*⁹¹. Ret is a receptor tyrosine kinase important for glial-derived neurotrophic factor and neurturin signaling⁹¹ and is important for ENCC proliferation, migration, and differentiation³. When we unilaterally knock down *ret* we observe a significant reduction in ENCC area compared to the contralateral side and a standard control condition (**Fig. 2.3B,D**). This is consistent with the role of *ret* in other models such as zebrafish⁵² and mice⁹².

Second, we tested a pharmacological inhibitor of Ret, PP1^{93,94}, to see if this would result in reduced ENCC migration. We began treating embryos after neurulation was complete and the vagal neural crest began migrating at NF stage 25. Treatment with 1 μ M of the Ret inhibitor resulted in a significant absence of ENCCs in the gut at NF stage 40 with 26.2% gut migration area on average (**Fig 2.3C,E**). Treatment with lower doses also significantly reduced the area of ENCC migration as compared to the vehicle control DMSO although to a lesser extent. Therefore, we are able to model varying severities of HSCR through treatment with a dose curve of the Ret inhibitor PP1.

We further tested this model by inhibiting Ret from NF stages 25 to 45 with the same dose curve of PP1 as performed on ENCCs and observing effects on differentiated enteric neurons. When staining for HuC/D and Acetylated α -Tubulin, we notice a similar trend: as the dosage increases, we see fewer enteric neurons in the hindgut of stage 46 *Xenopus* tadpoles compared to the DMSO control (**Fig 2.3F**). This can be most clearly observed in the center of the coil which is the most rostral gut portion in each image. These enteric neurons also seem to be less densely populated along the length of the

gut when treated with PP1 compared to DMSO. However, gut coiling has developed normally, suggesting that enteric neurons may not be required for gut morphology.

Novel assay to study gut motility in *Xenopus*

Finally, we developed an assay to study the function of the enteric nervous system through assessing gut motility in *Xenopus*. Previous work in zebrafish leveraged the transparent nature of the animals in conjunction with small fluorescent beads to observe the rate of bead expulsion after feeding³⁷. These studies labeled the gastrointestinal tract as 4 discrete regions and quantified the number of beads in each at various time points³⁷. Although this offers information about specific areas of the gut that may have dysfunctional transit, it is relatively low throughput as each individual animal is imaged. Our goal was to develop an assay in which we could assess gut motility in a high-throughput way (**Fig 2.4A**). In this novel assay, *Xenopus* tadpoles are raised for 9 days at room temperature until they are NF stage 47 and have begun feeding. On the day of the assay, tadpoles are fed a mixture of their food, Sera Micron, and 6 μm green fluorescent beads for 2 hours. After they have finished eating, they are moved from plastic dishes into a mesh trough in a glass dish containing fresh 1/3 MR. To wash the food out of the media, a vacuum is applied to one end of the dish to slowly remove the current media while pouring fresh 1/3 MR in from the opposite side. We found that if you move the entire mesh trough to new media and expose the tadpoles to air, they greatly increase the amount of excrement in the next stage of the assay, skewing the results. After the media is cleaned, the tadpoles are moved from the trough into a 6-well plate containing basket inserts with a plastic pipette that has been cut at the end to widen the

tip and not hurt the animals. 20 tadpoles are moved into each well and left to excrete for 3 hours. At the end of this time, the baskets are lifted from the wells to remove all the tadpoles at once while leaving the excrement with fluorescent beads in the wells. After the excrement has all settled to the bottom of the dishes overnight, the plates are tile-imaged on a wide-field microscope and the number of fluorescent beads per well is counted in FIJI.

To test this assay and identify modulators of gut motility, we performed a screen using 33 compounds from an FDA-approved drug library (**Fig 2.4B,C, Table 2.1**). We performed each drug treatment in triplicate such that 3 wells with 20 tadpoles each were treated with 10 μ M of one of the small molecules during the excretion portion of the assay. In total, 2040 tadpoles were treated in parallel. To identify hits in this screen, we chose a cutoff of DMSO \pm 1 standard deviation and have labeled the 3 largest positive and negative hits from the screen along with their mechanisms of action. Two of the hits, Donepezil and Darifenacin, both target acetylcholine signaling. Donepezil is an acetylcholinesterase inhibitor which increases gut motility by prolonging the duration of action of acetylcholine at the neuromuscular junction⁹⁵. In contrast, Darifenacin is an acetylcholine receptor antagonist, blocking the effects of acetylcholine on smooth muscle^{95,96}. The two other negative modulators are glipizide and vinblastine, which stimulate insulin release and stabilize microtubules respectively, both of which have been shown to reduce gut motility^{97,98}. Finally, the last two positive modulators are clomipramine and amoxapine, both serotonin and norepinephrine agonists, which were expected based on serotonin's well-known role in gut motility⁹⁹.

Discussion

Here we have shown that *Xenopus* is a novel model for studying the development and function of the enteric nervous system in the context of disease. We demonstrate that *phox2b* is a reliable marker for ENCCs and describe two parallel assays for quantifying ENCC migration. We further describe the development of mature neuronal organization using antibodies against HuC/D and Acetylated α -Tubulin to mark neuronal cell bodies and their projections respectively. We observe that the enteric nervous system in *Xenopus* develops in a similar trajectory to the human midfetal ENS¹⁰⁰. To test our model, we perturbed the function of the Hirschsprung's Disease risk gene *ret* in two ways and show that it is required for ENCC migration in *Xenopus* and later during enteric neuron maturation. Finally, we develop a novel gut transit assay to investigate modulators of gastrointestinal transit in a high throughput manner and find that dual serotonin/norepinephrine agonists increase gut motility.

This work builds on *Xenopus* as a model, adding another context in which the frog can be leveraged to study developmental processes. Previously avians, rodents, and zebrafish have been used to examine enteric neuron biology. Although they each have their respective strengths, *Xenopus* has clear advantages which we describe here. *Xenopus* has highly conserved developmental biology and has historically been used in key discoveries involving embryonic patterning, cell cycle control, and developmental signal transduction⁶⁵. Its high fecundity and ease of microinjections and drug treatments make high throughput experiments possible. More specific to the ENS, the same markers that are used to visualize ENCCs and enteric neurons in other vertebrates can be used in this model as well. An advantage of the *Xenopus* system is the ability to

unilaterally knockdown a gene and compare to its contralateral control which can reveal slight differences that may be missed when comparing between individuals with different genetic backgrounds. Here we have shown that knocking down *ret* decreases ENCC migration and provides the platform to knock down other disease risk genes to investigate their roles in this process. Additionally, we can assess differentiated neuron populations at later stages in development and compare neuronal subtype populations. Although we have performed these experiments in *Xenopus laevis*, the ENCC and enteric neuron staining experiments can be performed in *Xenopus tropicalis* as well, which opens the door to easier genetic manipulation with CRISPR/Cas9 in addition to morpholinos. Productive areas of improvement include the expansion to live imaging of ENCC migration, which could be performed with transgenic animals or microinjection of fluorescently-tagged mRNA into the blastomere contributing to the neural crest^{69,70}.

One of the biggest contributions of this work to the ENS field is the novel gut motility assay which allows for a high-throughput study of gut transit effectors. Current models offer a medium to low-throughput assay, such as in zebrafish³⁷, or a low-throughput *ex vivo* experiment as seen in rodent models⁵⁴. Our work describes the ability to study gut motility *in vivo* and the capability to screen many conditions in parallel. However, it remains to be explored how genetic knockdowns or germline mutant animals can be used in this assay. Future work should also develop methods for using the *tubb2b:GcAMP6s* transgenic animals¹⁰¹ to investigate enteric neuron activity during spontaneous peristalsis at NF stage 46.

Other open questions remain about ENS biology in *Xenopus* more broadly. The coiled nature of the *Xenopus* gut along with the defined cell fate maps offer the opportunity to

probe how enteric neurons migrate and differentiate during gut coiling. Future research could investigate whether ENCCs migrating from each side of the animal remain separate through gut development and what processes determine the timing of migration¹⁰¹. Our observation of circular tubulin-marked cells in the gut also warrants further exploration. As a first step we would like to test whether these cells are Sox10-positive, demonstrating if they are neural crest-derived. Further work could also image these cells live to determine whether they are migrating through the gut and if they eventually differentiate into enteric neurons. Both targeted injections of fluorescently-tagged tubulin and transgenic *Xenopus* lines would be helpful in testing these hypotheses. The neuronal subtypes in the *Xenopus* gut must also be further explored. Although previous work has described a subset of the neurochemical coding, it has not been extensive. The *Xenopus* model offers the opportunity to study the effect of perturbations on the distribution of neuronal subtypes, but this requires a better understanding of the neuronal populations and their developmental timing.

In summary, this work has demonstrated that the *Xenopus* model invites new questions in how the enteric nervous system develops. It is a genetically tractable system that can be used to study ENCC migration, enteric neuron differentiation, and ENS function. We have shown that this system is capable of modeling ENS diseases such as Hirschsprung's Disease, offering the opportunity to study the effects of other disorders on ENS development in the future.

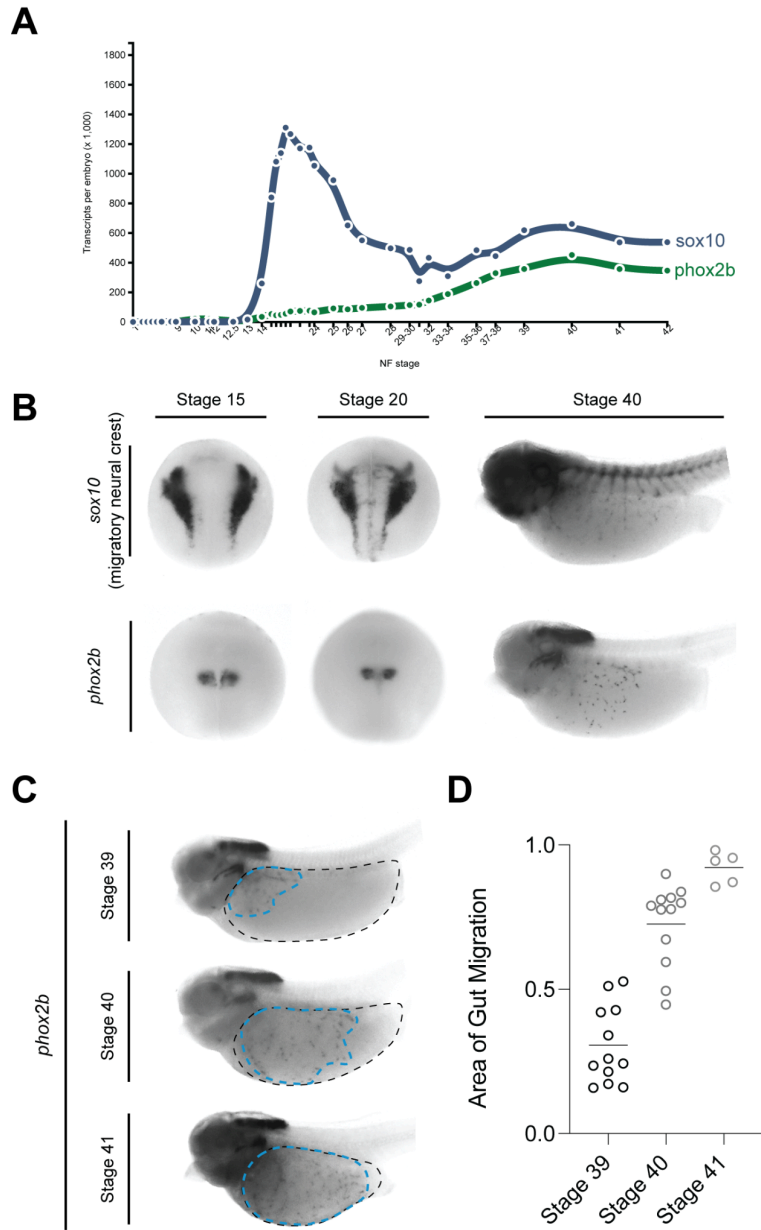


Figure 2.1. *phox2b* reliably marks enteric neuron progenitor cells in *Xenopus*.

(A) *sox10* and *phox2b* transcripts have similar expression slopes, increasing from stages 33 to 42. (B) RNA *in situ* hybridization staining for *sox10* and *phox2b* show expression in the early neural crest and neural tube as well as puncta in the gut at stage 40, demarcating ENCCs. (C) ENCCs migrate through the majority of the gut before coiling between stages 39 and 41. (D) Quantification of ENCC area compared to gut area by stage.

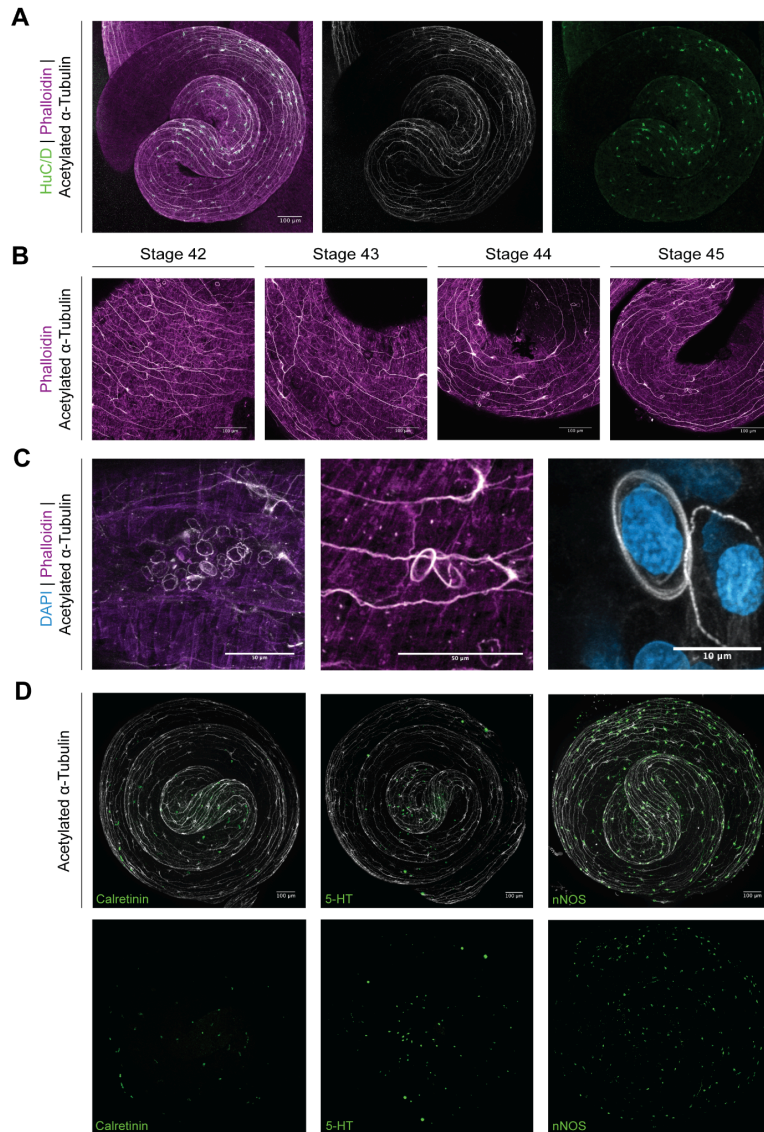


Figure 2.2. Enteric neuron organization is similar between *Xenopus* and humans
 (A) Stage 45 *Xenopus* enteric nervous system visualized by HuC/D (green, neuron bodies), Acetylated α -Tubulin (white, neuron bodies and projections), and phalloidin (magenta, gut muscle). (B) Enteric neuron organization becomes striated over developmental time from stage 42 to 45. (C) Circular cells visualized by Acetylated α -Tubulin in stage 45 *Xenopus* guts occasionally appear in groups and along neural projections. (D) Stage 46 *Xenopus* gut contains Calretinin+, 5-HT+, and nNOS+ cells (green).

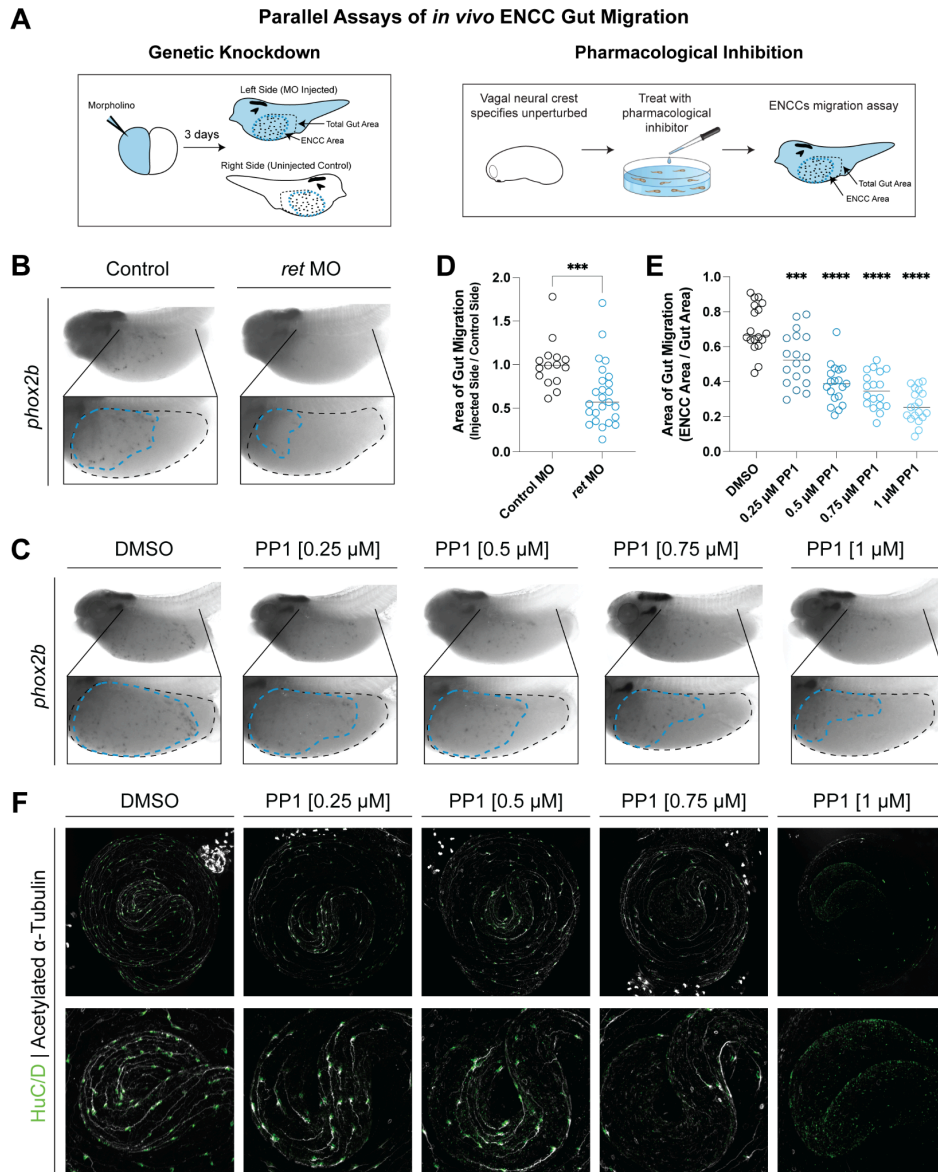


Figure 2.3. Hirschsprung’s Disease risk gene *ret* is required for ENCC migration in *Xenopus*.

(A) Schematic of parallel assays to assess *in vivo* gut migration in *Xenopus*. Target gene expression can be unilaterally knocked down at the 2 cell stage and later compared against the contralateral control side. Target proteins can be inhibited after the vagal neural crest begins migrating at stage 25 to bypass early effects on neural crest specification. (B) Perturbation of HSCR risk gene *ret* results in reduced ENCC migration. (C) Treatment with Ret inhibitor PP1 results in reduced ENCC migration that is dose-dependent. (D) Area of gut migration quantification in *ret* and control MO conditions. Control MO in gray, *ret* MO in blue. A one-tailed Mann-Whitney test was performed, $p = 0.0004$. (Figure caption continued on the next page.)

(Figure caption continued from the previous page.) (E) Area of gut migration quantification in PP1 and DMSO conditions. DMSO in gray, PP1 doses in blue. A One-Way ANOVA was performed followed by a Tukey test to adjust for multiple comparisons. p values are compared to DMSO, ***p_{adj} = 0.0003 and ****p_{adj} < 0.0001.

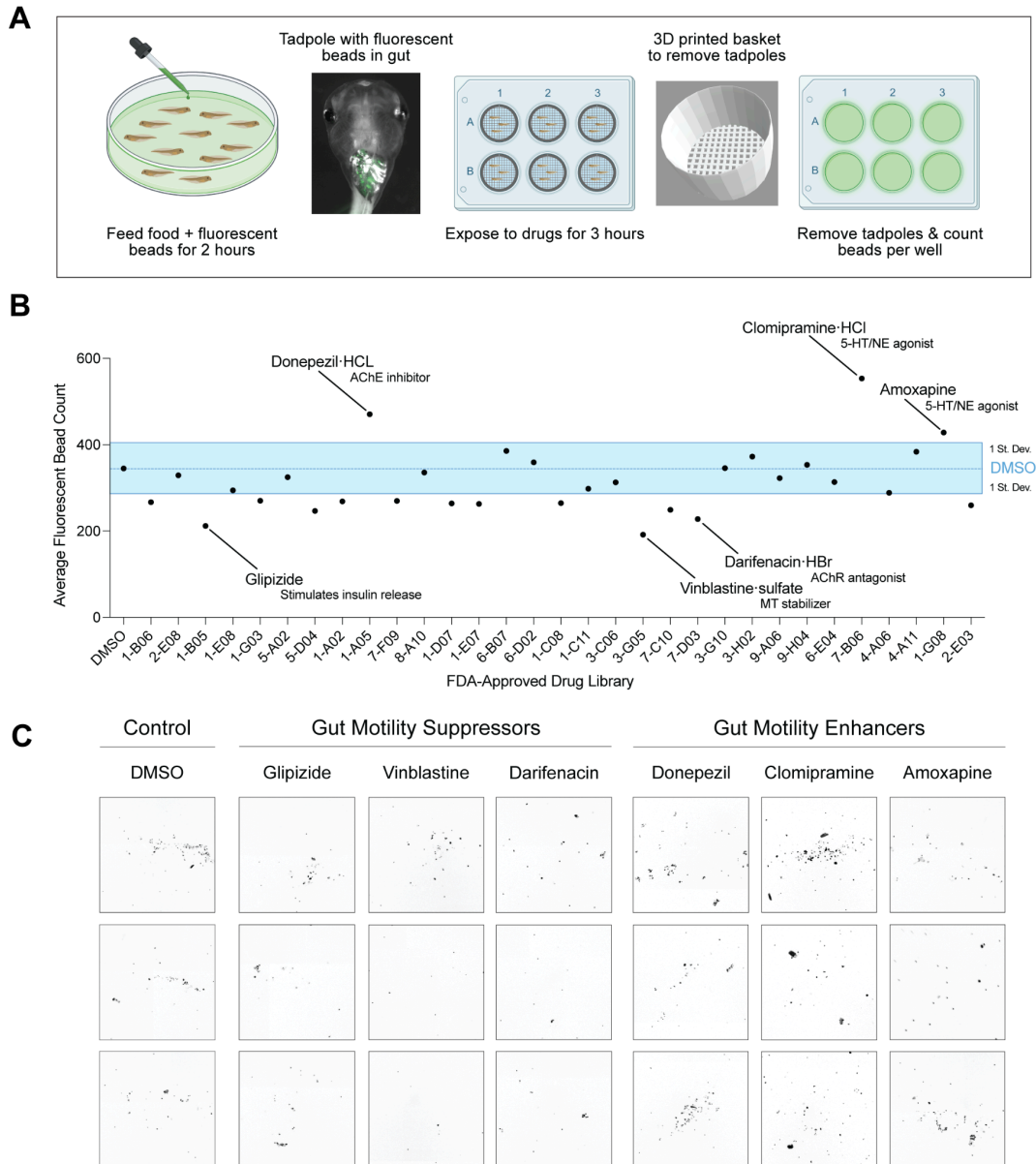


Figure 2.4. Gut motility screen in *Xenopus* identifies modulators of gastric motility.

(A) Schematic of the *in vivo* gut motility assay. At NF stage 47, tadpoles were fed food with fluorescent beads for 2 hours, then placed in a 6-well plate in 3D-printed baskets with 20 animals/well for 3 hours. Tadpoles are then removed by taking out baskets and leaving excrement with fluorescent beads behind, after which the plates were imaged to count the number of beads per well. Created with BioRender.com. (B) Small molecule screen identifies modulators of gut motility. Dotted blue line at DMSO average, blue box around 1 standard deviation above and below DMSO average. (C) Representative images of fluorescent beads (false-colored black).

Table 2.1. Gut motility drug screen results. Fluorescent bead counts for each FDA-approved small molecule tested in the screen.

KEY	CONTROL				
	SUPPRESSOR				
	ENHANCER				
ID	CAS	Drug Name	MW	Mechanism of Action	Mean Bead Count
		DMSO		Vehicle control	345.6666667
1-B06	73-05-2	Phentolamine HCl	317.8	Alpha-adrenergic blocker	236.6666667
2-E08	5786-21-0	Clozapine	326.8	Serotonin antagonist	346
1-B05	29094-61-9	Glipizide	445.5	Potassium channel blocker	217
1-E08	139264-17-8	Zolmitriptan	287.4	Serotonin 1B/1D agonist	301.6666667
1-G03	66357-59-3	Ranitidine-HCl	350.9	Histamine H2 antagonist	279
5-A02	6493-05-6	Pentoxifylline	278.3	Phosphodiesterase inhibitor, adenosine receptor antagonist	277
5-D04	22204-88-2	Tramadol-HCl	299.8	Opioid receptor agonist	246.6666667
1-A02	21462-39-5	Clindamycin-HCl	461.4	Antibiotic	268.6666667
1-A05	120011-70-3	Donepezil-HCl	416	Acetylcholinesterase inhibitor	470.6666667
7-F09	62-31-7	Dopamine-HCl	189.6	Dopamine agonist	269.6666667
8-A10	153439-40-8	Fexofenadine-HCl	538.1	Histamine H1 antagonist	335.6666667
1-D07	10347-81-6	Maprotiline-HCl	313.9	Norepinephrine agonist	264
1-E07	16676-29-2	Naltrexone-HCl	377.9	Opioid receptor antagonist	263
6-B07	122852-69-1	Alosetron-HCl	330.8	Serotonin 3 antagonist	385.6666667
6-D02	82248-59-7	Atomoxetine-HCl	291.8	Norepinephrine reuptake inhibitor	359.3333333
1-C08	6190-39-2	Dihydroergotamine Mesylate	679.8	Serotonin 1D agonist	264.6666667
1-C11	58-08-2	Caffeine	194.2	Adenosine A1/A2A antagonist	298
3-C06	115956-12-2	Dolasetron	324.4	Serotonin 3 antagonist	313
3-G05	143-67-9	Vinblastine sulfate	909.1	microtubule stabilizer	191.6666667
7-C10	14663-23-1	Dantrolene sodium	336.2	Muscle relaxant	249.3333333
7-D03	133099-07-7	Darifenacin-HBr	507.5	acetylcholine receptor antagonist	227.6666667
3-G10	33386-08-2	Buspirone-HCl	422	Serotonin antagonist, noradrenaline/dopamine agonist	345.6666667
3-H02	298-46-4	Carbamazepine	236.3	Blocks use-dependent sodium channels	372.6666667
9-A06	72-33-3	Mestranol	310.4	Estrogen agonist	322.6666667
9-H04	58-39-9	Perphenazine	404	Dopamine D1/D2 antagonist	353.3333333
6-E04	132-17-2	Benztropine mesylate	403.5	Muscarinic acetylcholine receptor antagonist, dopamine agonist	313.6666667
7-B06	17321-77-6	Clomipramine-HCl	351.3	Serotonin/Norepinephrine agonist	553.3333333
4-A06	4682-36-4	Orphenadrine citrate	461.5	Histamine H1 antagonist, NMDAR antagonist	288.6666667
4-A11	17230-88-5	Danazol	337.5	Estrogen antagonist	383.6666667
1-G08	14028-44-5	Amoxapine	313.8	Serotonin/Norepinephrine agonist	428.3333333
2-E03	63-92-3	Phenoxybenzamine-HCl	340.3	Alpha-adrenergic receptor antagonist	259.6666667

Materials and Methods

***Xenopus* husbandry**

Xenopus laevis adults originated from the National *Xenopus* Resource Center¹⁰¹. Animals used were of wildtype lines of both sexes. Animals were housed in a recirculating system and were maintained in accordance with approved UCSF IACUC protocol AN199587-00A. Ovulation was induced with human chorionic gonadotropin (Sigma CG10), and embryos were collected and manipulated according to standard procedure¹⁰². The *Xenopus* community resource Xenbase was referenced daily⁸⁷.

***Xenopus* microinjections and loss of function**

A Narishige micromanipulator, Parker or Narishige Picospritzers, and Zeiss Stemi508 microscopes were used to microinject reagents into 1 cell of 2-cell stage embryos. For morpholino injections, 4.2 nl injection volume of each condition was measured using an eyepiece micrometer, delivering 14 ng of the morpholino per blastomere. Embryos were injected and grown at 21°C in 1/3 Modified Ringer's (MR) solution. A translation-blocking *ret* morpholino (5' AAAGTTGCCCTCTGCAATAATCCA 3', GeneTools) was compared against a standard control morpholino (5' CCTCTTACCTCAGTTACAATTTATA 3', GeneTools).

Whole-mount RNA *in situ* hybridization

All embryos were fixed in MEMFA for 1 hour and stained according to Willsey et al 2021¹⁰³ using anti-DIG (1:3000, Sigma 11093274910) and BM Purple (Sigma 11442074001). *phox2b* probe plasmid was a kind gift from the Harland lab (IMAGE clone #8956276, probe synthesis with T7 enzyme and EcoR1 restriction enzyme), and

sox10 probe was previously described⁷¹. The stainings were performed in a high-throughput basket format with 200 µm mesh in 3D-printed racks^{103,104}. All embryos were imaged on a Zeiss AxioZoom.V16 with a 1x objective and extended depth of focus processing in Zeiss Zen software.

Immunofluorescence staining

For NF stage 45 samples immunostaining was performed according to Willsey et al 2021¹⁰³ with the omission of the bleaching step as it was found to add bubbles that affected GI morphology. Phalloidin (1:400, Life Tech A34055) and DAPI (1:400) were added during the secondary antibody step. Primary antibodies used were against Acetylated α -Tubulin (1:200, Abcam ab179484), HuC/D (1:100, Life Technologies A-21271), Calretinin (1:100, Swant CR7697), 5-HT (1:100, ImmunoStar 20080), nNOS (1:100, abcam AB5586-1001), and Tyrosine hydroxylase (1:100, Neta Scientific MILL-AB152). Secondary antibodies (Abcam ab150177, Thermofisher A32733) were diluted at 1:250. Embryos were imaged on a Zeiss 980 LSM with a 10x air or 63x oil objective and Airyscan processing. Whole gut neuron subtype samples were imaged on a Zeiss AxioZoom.V16 with a 1x objective and a Zeiss 506 monochrome camera and apotome. Maximum intensity projections were performed in Zen.

Drug treatment

Ret inhibitor (PP1, Sigma P0040) was resuspended in DMSO at 1 mM. Embryos were treated with drug or an equal volume of DMSO diluted in 1/3 MR at NF stage 25 and fixed at NF stage 40 for RNA *in situ* hybridization staining for ENCC migration assay or at NF stage 45 for immunofluorescence staining. Media was not refreshed while embryos were growing.

Gut motility assay

All gut motility assays were performed in *Xenopus laevis*, since pilot studies showed they excrete more than *X. tropicalis* (they are larger animals), which was enough to be able to reliably quantify bead number per well from 20 animals. Since these experiments are all drug treatments and not genetic perturbations, the advantages of the *X. tropicalis* diploid genome are less critical. *Xenopus laevis* embryos were collected and raised for 9 days at room temperature until NF stage 47. At the beginning of the gut motility assay, tadpoles were moved into 15 cm dishes containing 20 mL of 1/3 MR. Food was prepared by resuspending 1 g of sera micron (Sera 00720) in 45 mL of 1/3 MR with 30 μ L of 6 μ m fluorescent bead solution (Polysciences 18862-1) added, similarly to what has previously been used to assay gut motility in zebrafish³⁷. 2.5 mL of the food suspension was added to each 15 cm dish for each condition. Tadpoles were left to feed for 2 hours and then rinsed in a homemade mesh (Spectra Mesh 100 μ m and 200 μ m, 146488 and 146487) trough in a glass dish (Grainger 900203). Using a vacuum, media was removed while fresh 1/3 MR was added until the media was clear of food and beads. Tadpoles were moved from the mesh trough using a plastic pipette into a fresh 15 cm dish. They were then transferred to a 6-well plate with homemade 3D-printed baskets with lattice bottoms inserted into each well. 20 tadpoles were allotted into each basket. After defecating for 3 hours, baskets with tadpoles were removed from each well, leaving excretion with fluorescent beads in the well. All plates were left in the dark at 4°C overnight to let all matter sink to the bottom of the plate. Then, plates were tile-imaged in the same position on a Zeiss AxioZoom.V16 with a 1x objective and analyzed in Fiji.

Tadpoles were raised only in 1/3 MR until the 3-hour defecation period, at which point they were acutely exposed to 10 μ M of each compound individually. Small molecules selected from an FDA-approved drug library (Enzo Life Sciences BML-2843-0100) were tested at 10 μ M alongside an equal volume of DMSO diluted in 1/3 MR.

Image Processing and Statistical Analyses

All images were processed in FIJI (NIH) and arranged in Illustrator (Adobe). For ENCC quantification, the area of ENCCs and total gut area were both measured by drawing with the free-hand selection tool and quantified with the measure function. The ENCC area was normalized to the total gut area. Tests for normality were performed in Prism (GraphPad) followed by an ANOVA or Kruskal-Wallis test as appropriate. For unilateral mutagenesis, multiple paired t tests were performed to compare the uninjected and injected sides of each embryo per condition and then adjusted for multiple comparisons with the Holm-Šídák method. For small molecule experiments, a one-way ANOVA or Kruskal-Wallis test was used as appropriate based on normality tests, followed by an unpaired t test or a Wilcoxon rank-sum test.

For gut motility image analysis, tiled images were analyzed in FIJI with a macro to Find Maxima (Prominence > 60, Output type: Count) in each well of a 6-well plate. Counts were imported into Prism and standard deviation was calculated for control treatments. For comparing between DMSO, TG003 and rescue treatments, all conditions passed normality and a one-way ANOVA was performed followed by unpaired one-tailed t tests with Welch's correction.

CHAPTER 3

Autism gene variants disrupt enteric neuron migration and cause gastrointestinal dysmotility

Introduction

Autism Spectrum Disorders (ASD) are neurodevelopmental disorders defined by atypical social interactions, repetitive behaviors, and restricted interests²². One of the most prevalent and impairing comorbidities of ASD is gastrointestinal (GI) distress, commonly presenting as gastric motility symptoms like constipation, diarrhea, or abdominal pain¹⁹⁻²¹. Despite this well-established comorbidity, the underlying molecular mechanisms remain unknown. The discovery of high-confidence (hc), large-effect autism genes³¹ has opened the door to studying these genes *in vivo* in order to identify the molecular origins of this co-occurrence. In the central nervous system, hcASD risk genes have been shown to converge in regulating the development of neural progenitor cells^{30,71,105-110}, motivating the hypothesis that these genes may also contribute to the development of the enteric nervous system (ENS), the neurons that control the GI tract. Indeed, the role of one of the first identified large-effect autism genes, *CHD8*, has been elaborated in zebrafish, where disruption of *chd8* caused reduced colonization of enteric neurons into the gut as well as gut dysmotility³⁵. Consistently, it has been shown that autism genes are enriched in expression in human adult enteric neurons⁹, the neurons controlling gastric motility¹¹¹. Together, these findings raise the possibility that the observed comorbidity may be due to atypical development of the ENS.

Here we document the prevalence of GI dysmotility in patients with pathogenic variants in hcASD genes, highlighting dysmotility, consistent with potential ENS dysfunction. These genes represent a wide swath of functional annotations and are highly pleiotropic, complicating efforts to establish direct links between molecular mechanisms and observed phenotypes^{33,112,113}. A convergence neuroscience approach, where many genes are studied empirically in parallel and phenotypes and functions in common to multiple genes are considered more likely to be relevant to core biology, is one avenue to combat this challenge^{33,112,113}. With this strategy in mind, we chose the model organism *Xenopus tropicalis* to study five hcASD genes representing disparate functional annotations *in vivo* to identify convergent phenotypes in the development of the ENS. These five genes include several with functional annotations in neurotransmission (*SYNGAP1*, *SCN2A*), gene expression regulation (*CHD8*, *CHD2*) and kinase activity (*DYRK1A*)³⁰. These frogs have a simple diploid genome very similar to that of humans^{68,114}, an elaborate, coiled GI system⁷⁶, and the ability to perform unilateral genetic perturbations within an animal^{68,71–73,115}.

For all five gene perturbations individually (*SYNGAP1*, *CHD8*, *SCN2A*, *CHD2*, or *DYRK1A*), we observe defects in embryonic enteric neuron progenitor migration. We further focus on the hcASD gene *DYRK1A*, which encodes a kinase, and show that it is also required for gut motility *in vivo*. With a targeted drug screen we identify the selective serotonin reuptake inhibitor escitalopram and a serotonin receptor 6 agonist that can each individually ameliorate this dysmotility. Together, these results suggest that ENS developmental defects may be a convergent, contributing factor to the

comorbidity between autism and GI distress and that increasing serotonin signaling may be a productive therapeutic strategy.

Results

hcASD gene expression is enriched in enteric neurons and their progenitors

Previously, hcASD gene expression has been shown to be enriched in adult human enteric neurons⁹. To assess hcASD gene expression in this tissue during development, we analyzed scRNA sequencing data from a range of stages during human prenatal gut development¹¹⁶. All 252 hcASD genes with an FDR < 0.1³¹ were expressed in the data set. We used Module Score Analysis (AddModuleScore, Seurat R Package) to calculate the average expression of these genes and their relative expression enrichment across cell types, compared to a comparably expressed random control geneset (**Fig. 3.1A-B**). hcASD gene expression enrichment was significantly higher in enteric neurons and their progenitors, enteric neural crest-derived cells (ENCCs), compared to all other cell types in the developing human prenatal gut (**Fig. 3.2, Fig. 3.3**, $p_{adj} < 0.0001$ and $p_{adj} < 0.0001$, Kruskal-Wallis test followed by Wilcoxon Rank-Sum tests with Bonferroni adjustment for multiple comparisons). These results suggest that hcASD gene expression is enriched in both mature and developing enteric neurons.

Prevalence of GI dysmotility among patients with hcASD gene variants

Recently Simons Searchlight has compiled caregiver survey data for patients with large-effect variants in autism-associated genes and loci, as well as often for unaffected family members¹¹⁷. Within these data, we identified any patient with a genetic variant in one of the 252 hcASD risk genes. Nineteen genes were represented, with sixteen

genes having more than ten affected individuals. Of these sixteen genes, seven are within the ten highest-associated hcASD genes (FDR < 0.01; *SYNGAP1*, *CHD8*, *ADNP*, *SCN2A*, *FOXP1*, *CHD2*, *GRIN2B*)³¹. All sixteen patient cohorts had caregiver-reported GI symptoms (average prevalence = 51.7%), while few unaffected family members did (average prevalence = 0.4%) (**Fig. 3.2C**). To dive more deeply into the specific nature of these GI symptoms, we identified any patient in the Ciitizen[®] medical record database with a genetic variant in a hcASD gene. Medical record data were available for 5 hcASD genes: *SYNGAP1* (n = 186 patients), *SCN2A* (n = 58 patients), *CHD2* (n = 41 patients), *SLC6A1* (n = 49 patients), and *STXBP1* (n = 80 patients). For all of these cohorts, over 80% of individuals had medical record diagnoses related to GI symptoms (**Tables 3.1-3.5**), consistent with caregiver reports for similar cohorts in Simons Searchlight described above. Of these diagnoses, GI dysmotility symptoms, particularly constipation, were reported in medical records for over 60% of individuals among all cohorts (**Fig. 3.2D-E**). Since GI motility is controlled by the ENS¹¹⁸, these observations are consistent with the possibility that variants in these genes disrupt ENS development and/or function, leading to gut dysmotility.

hcASD gene variants disrupt ENS migration *in vivo*

Next we next aimed to examine the role of hcASD genes in the development of the ENS *in vivo*. ENS progenitors (ENCCs) are exclusively derived from the neural crest and migrate into the gut during embryonic development⁵. To study the role of hcASD genes in the development of these cells *in vivo*, we adapted the vertebrate diploid frog model *Xenopus tropicalis*, where parallel *in vivo* analysis of hcASD genes during embryogenesis is possible. Specifically, we visualized the ENCCs by whole-mount RNA

in situ hybridization for their marker gene *phox2b*^{84,111} (**Fig. 3.4A**) during embryogenesis following perturbation of hcASD genes by unilateral CRISPR/Cas9 mutagenesis, comparing the mutated half of the animal to the contralateral control side (**Fig. 3.4B**). We chose to perturb 5 of the 20 highest-associated hcASD genes³¹ with disparate functional annotations (neurotransmission: *SYNGAP1* and *SCN2A*, chromatin regulation: *CHD2* and *CHD8*, and kinase activity: *DYRK1A*) by individually injecting Cas9 protein with an sgRNA into one cell of two-cell stage embryos. We have previously validated these sgRNAs in *X. tropicalis* for their loss-of-function efficiency^{71,72}. We hypothesized that phenotypes observed in all of these five mutants are more likely to be relevant to the core underlying biology of the ASD/GI comorbidity, and less likely to be a byproduct of pleiotropy. The phenotype we observed for all five gene perturbations was a significant reduction in ENCC migration area, which was not observed in control animals injected with Cas9 protein and a sgRNA targeting a pigmentation gene *slc45a2* (**Fig. 3.4C-D, Fig. 3.5**). This result was comparable for all five hcASD gene perturbations, irrespective of the gene's annotated cellular function, suggesting functional convergence in the process of ENCC migration.

Depletion of *dyrk1a* disrupts neural crest development and ENCC migration

Next we elaborated this finding for *dyrk1a* in *Xenopus*, given our previous experience perturbing this gene within the central nervous system and the abundance of associated molecular tools^{71,72,119,120}. We observed that *dyrk1a* is expressed in ENCCs during migration (**Fig. 3.6A**) and persists in mature enteric neurons (**Fig. 3.6B-C, Fig. 3.3**), particularly at the primary cilium, an organelle required for ENCC migration¹²¹. As additional validation that our CRISPR-mediated disruption of *dyrk1a* was specific to this

gene, we also perturbed *dyrk1a* with a validated translation-blocking morpholino^{72,119} and observed the same phenotype as the CRISPR perturbation (**Fig. 3.7A-B**). This is particularly important since CRISPR/Cas9 gene editing in *Xenopus* F0 embryos often results in a mosaic, less severe phenotype⁶⁷, and it is possible that this mosaicism may result in unedited cells mitigating the migration phenotype since enteric neural crest-derived cells have been shown to migrate in chains⁸.

ENCCs develop exclusively from the neural crest^{3,5}, and our group and others have observed *dyrk1a* expression in the *Xenopus* neural crest^{72,119,120}. Therefore, this migration phenotype could be due to earlier neural crest developmental defects. Indeed, by CRISPR or morpholino perturbation, we observed defects in the early neural crest marker *sox10*^{122,123} at NF stage 15 by whole-mount RNA *in situ* hybridization (**Fig. 3.8A**). This indicates that *Dyrk1a* is required earlier in the embryo for neural crest development, a finding that is corroborated by a recent study¹²⁰. To test whether other hcASD genes may also affect neural crest development, we knocked down the expression of *syngap1*, *chd8*, *scn2a*, or *chd2* and assayed *sox10* expression. We observed significant defects following depletion of *chd8* and *chd2*, a moderate effect for *syngap1*, and no effect for *scn2a* (**Fig. 3.9**).

Next we aimed to separate the early requirement of these genes in neural crest development from any later roles in ENCC migration. To do this, we took advantage of the ability to conditionally inhibit *Dyrk1a* by pharmacological inhibition after neural crest specification is complete, at the onset of vagal neural crest migration⁴⁸ (**Fig. 3.7A-B, Fig 3.8B**). When we inhibited *Dyrk1a* with either TG003 or harmine¹²⁴ at the onset of migration (NF stage 25), ENCC migration was still disrupted and to a similar extent as it

was by CRISPR perturbation, or compared to our positive control Ret inhibitor, a model of Hirschsprung's Disease^{125,126} (**Fig 3.8C-D**). This was in contrast to the negative control treatments DMSO or moclobemide, a MAO inhibitor that controls for a potential off-target effect of harmine¹²⁷. Together, these results suggest that *dyrk1a*, while required for early neural crest development, is also independently required for ENCC migration in *Xenopus*.

Depletion of *dyrk1a* decreases gut motility *in vivo*

We next assessed whether inhibition of Dyrk1a during development affects gut motility *in vivo*. As seen above, gut dysmotility in the form of constipation is common among patient cohorts for several hcASD risk genes. To assess gut transit in *Xenopus*, we developed an *in vivo* gut motility assay where mature tadpoles (NF stage 47) were fed food with 6 μ m fluorescent beads for 2 hours, rinsed out of the food and placed in baskets in 6-well plates to defecate for 3 hours, and then taken out by removing the baskets while leaving the excrement and fluorescent beads behind (**Fig. 3.7C**). The plates were then imaged with a fluorescence microscope and the number of fluorescent beads per well was counted in Fiji. Each well contained 20 tadpoles and each condition was completed in triplicate. To test the role of Dyrk1a in gut motility *in vivo*, we raised animals in the Dyrk1a inhibitor TG003 or in control DMSO solution (starting at NF stage 20) and then performed the *in vivo* gut motility assay at mature tadpole stage (NF stage 47). There was a significant decrease in the number of fluorescent beads excreted in animals treated with the Dyrk1a inhibitor, compared to the DMSO control-treated tadpoles ($p = 0.002$, Wilcoxon Rank-Sum test) (**Fig. 3.7D-E**). This result suggests that developmental Dyrk1a inhibition *in vivo* causes gut dysmotility in *Xenopus* tadpoles.

Serotonin reuptake inhibitor treatment rescues gut dysmotility following Dyrk1a inhibition

Serotonin signaling is known to control enteric neuron activity and gut motility⁹⁹. Therefore, we selected 8 FDA-approved drugs that impact serotonin signaling at various points in the pathway (**Fig. 3.10A**) and tested whether acute treatment alters gut movement with our *in vivo* gut motility assay in unmanipulated mature tadpoles. Of these drugs, at the concentration we tested (10 μ M), only the selective serotonin reuptake inhibitor (SSRI) escitalopram oxalate was able to promote gut motility greater than 1 standard deviation compared to negative control treatment DMSO (**Fig. 3.10B**). Escitalopram oxalate (also known as Lexapro) is a common SSRI that interacts with SERT, the serotonin transporter, to inhibit the reuptake of serotonin into the presynaptic cell, thereby prolonging serotonin pathway activation (**Fig. 3.10A**). This result is consistent with previous studies in which activating or prolonging active serotonin signaling promotes gut motility in mammals^{128–131}.

Next we tested whether this SSRI could acutely rescue the effects of developmental Dyrk1a inhibition on gut motility. In addition to this SSRI, we concurrently tested a more specific activator of serotonin signaling, an agonist for serotonin receptor 6 (5-HTR6) (WAY-181187¹³²). We included this drug because both Dyrk1a and serotonin receptor 6 specifically localize to primary cilia¹³³ (**Fig. 3.6C-D**). To test these compounds, we raised tadpoles in DMSO or TG003 (Dyrk1a inhibitor) and performed our *in vivo* gut motility assay, adding 10 μ M escitalopram oxalate or WAY-181187 to a portion of the TG003-treated animals acutely during the 3 hour excretion portion of the assay. Acute exposure to either of these compounds during the excretion portion of the assay (3

hours) rescued the decreased motility phenotype of the Dyrk1a inhibitor-treated animals, restoring excretion to that comparable to the DMSO control (**Fig. 3.10C-D**). Therefore, these results suggest that Dyrk1a-associated gut dysfunction can be ameliorated by acute treatment with an SSRI or, more specifically, with a 5-HTR6 agonist. Together, our work suggests a model (**Fig. 3.10E**) in which ASD genetic variants cause atypical ENCC development, leading to GI dysmotility, and suggests serotonin signaling as a potential therapeutic pathway.

Discussion

The co-occurrence of autism and GI issues is well-established¹⁹, yet the molecular mechanisms underlying this comorbidity remain unclear. Here we document the prevalence of GI issues in individuals with variants in hcASD genes, particularly highlighting constipation, a symptom of GI dysmotility. Our group and others have shown that many hcASD genes converge to regulate neuronal development in the central nervous system^{30,71,105–110}, motivating us to consider whether these genes also contribute to the development of the ENS. Consistently, we observe that hcASD gene expression is enriched in both enteric neurons and their migrating progenitor cells during human embryonic development. Therefore, to test this hypothesis, we use a vertebrate *in vivo* model to individually perturb five hcASD genes with disparate functional annotations (neurotransmission, chromatin regulation, kinase activity). We observe disrupted ENCC migration for each, suggesting that atypical ENCC migration may contribute to GI dysmotility in ASD. We further investigate the role of Dyrk1a in gut motility and observe that Dyrk1a perturbation leads to a decrease in excretion that can be restored by acute exposure to agonists of serotonergic signaling.

This work adds to a growing literature suggesting that variants in ASD genes perturb ENS development^{20,134}, consistent with work done in zebrafish for *CHD8*³⁵ and in mice for *FOXP1*³⁸ and *PTEN*³⁴. While a fish study of *SHANK3* did not observe a significant change in gut neuron number³⁷, this group did identify disrupted serotonergic signaling in the gut, consistent with our findings that manipulating serotonin signaling could be a potential therapeutic avenue. Indeed, the role of serotonin signaling in gut motility is well-established^{128–131}, so this pathway could be productively exploited in the context of ASD more broadly for treating GI issues. Moving forward, other key questions remain including how ASD gene variants affect enteric neuron number, differentiation, organization, morphology, and activity in mature animals. In particular, the role of cell death in these phenotypes will need to be explored, as we have previously shown that DYRK1A inhibition in the central nervous system causes apoptosis⁷². Additionally, our work here characterizing loss of function for these genes could be complemented by the use of heterozygous germline mutant animals to recapitulate the haploinsufficiency present in individuals with pathogenic *de novo* variants in these genes. Finally, intersecting these findings regarding ENS development with other proposed mechanisms of GI dysmotility in ASD, particularly since ENS developmental defects are known to impact the composition of the gut microbiome¹³⁵.

Impaired ENCC migration is a central observation of our study, consistent with previous work in an assembloid model suggesting that neuron migration may be a convergent process disrupted in neurodevelopmental disorders¹³⁶. Interestingly, we observed that ENCC migration is affected by perturbation of genes known for their roles in neurotransmission (*SYNGAP1*, *SCN2A*). Similar to our previous findings in *Xenopus*

central nervous system development⁷¹ that have been recently validated in human cortical organoids¹¹⁰, this work suggests that these genes may have additional roles beyond neurotransmission during ENS development. Recently, several of these neurotransmission proteins have been shown to localize to the cilium¹³⁷, an organelle known to be required specifically for ENCC migration into the gut¹²¹. Here we show that Dyrk1a localizes to the primary cilium in enteric neurons in *Xenopus* (**Fig. 3.6C**). It is also known that serotonin receptor 6 (5-HTR6) specifically localizes to the cilium in neurons¹³³. Here we show that acute exposure to a 5-HTR6 agonist is able to increase gut motility and rescue a Dyrk1a model of dysmotility. Given the role of serotonin in gut motility and development⁴⁰, a productive area of future investigation will be to understand how other ASD gene variants perturb primary cilia in the development and function of the ENS and whether SSRIs can affect gut motility in those genetic contexts as well.

In summary, this work documents the prevalence of gut dysmotility, particularly constipation, in many individuals with large-effect variants in hcASD genes. Disruption of five hcASD genes convergently impacts ENCC migration in *Xenopus*, and, based on the study of Dyrk1a, this disruption may underlie the gut dysmotility seen in affected individuals. It will be important future work to determine the extent to which perturbations of other hcASD genes also result in gut dysmotility, and whether serotonin activation can also ameliorate any observed phenotypes. If this finding holds for many hcASD genes, investigating the therapeutic potential of serotonin activation for restoring gut motility in affected individuals may be a productive endeavor.

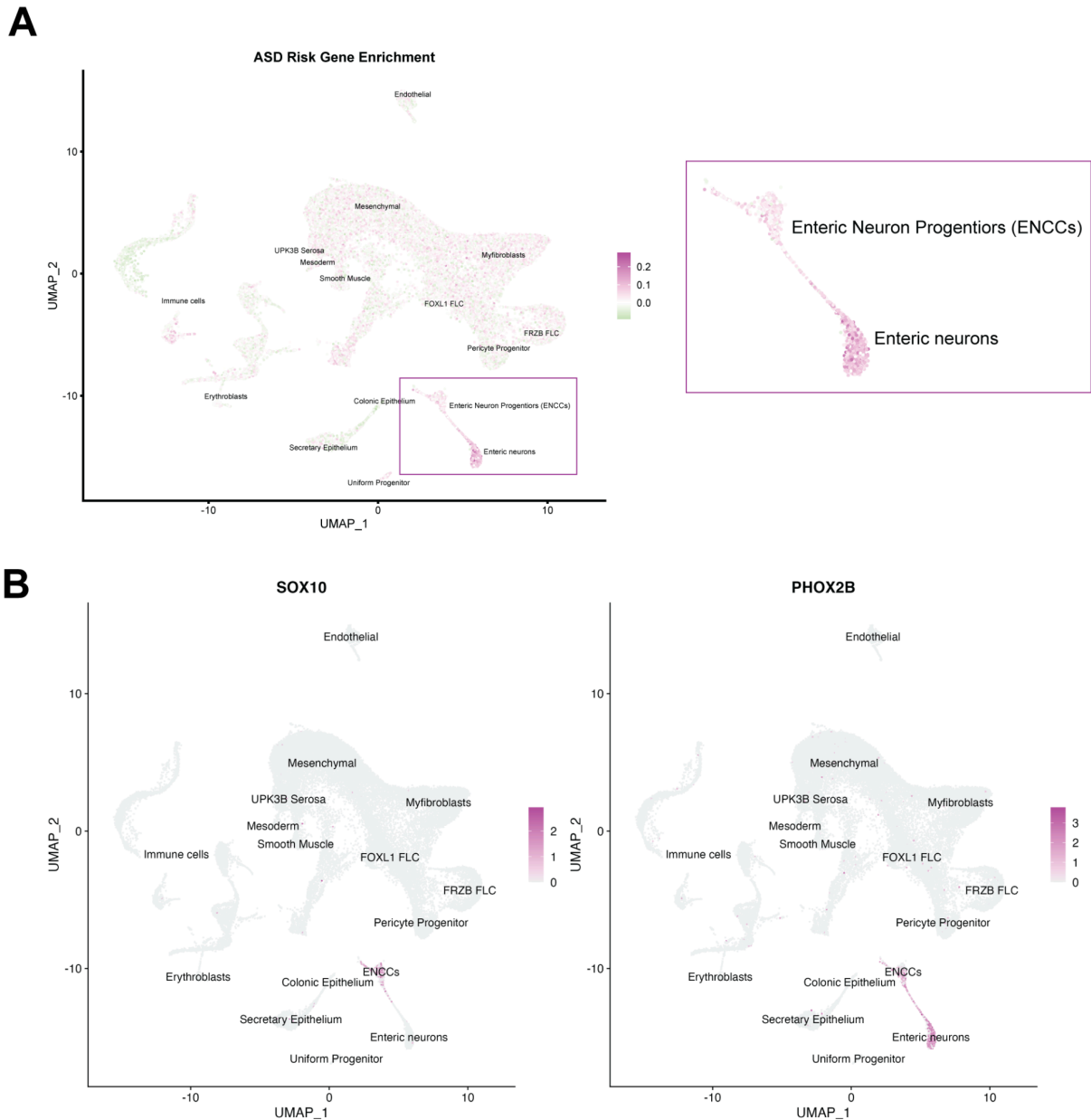


Figure 3.1. hcASD gene expression enrichment in human prenatal gut transcriptomic dataset¹¹⁶.

(A) UMAP of human prenatal gut scRNA-sequencing data¹¹⁶. Cells colored according to enrichment of hcASD gene module scores. Enteric neurons and ENCCs are outlined in a red rectangle and enlarged to the right. (B) The expression patterns of two marker genes *SOX10* (neural crest) and *PHOX2B* (vagal neural crest, ENCCs, and enteric neurons) to show cell-type identities for these populations.

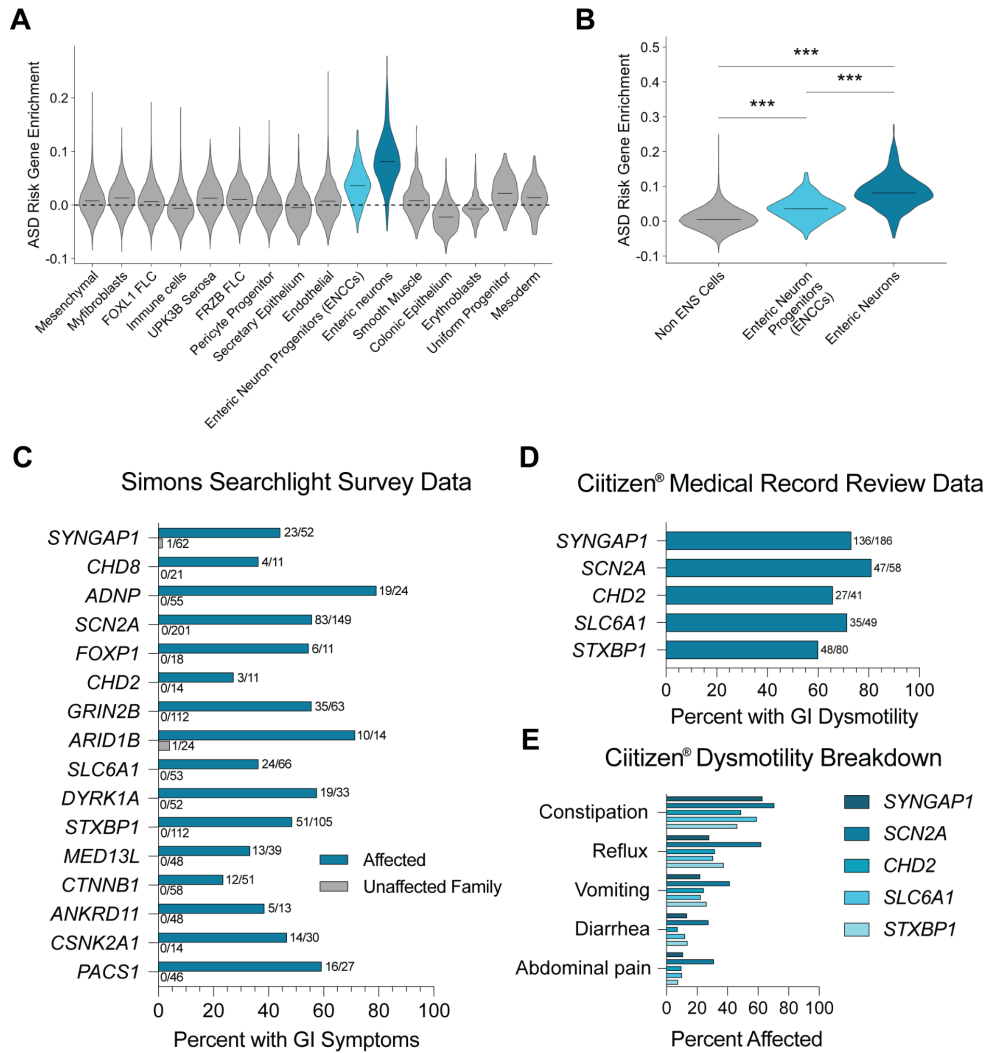


Figure 3.2. hcASD gene expression is enriched in ENS cells and individuals with pathogenic variants in these genes experience GI issues.

(A) Enrichment of 252 hcASD genes is higher in Enteric Neuron Progenitors (ENCCs) and Enteric Neurons compared to all other cell types in single-cell RNA-sequencing data from the human prenatal gut¹¹⁶. (B) 252 hcASD genes are enriched in ENCCs and Enteric Neurons compared to all other Non-ENS cells in the human prenatal gut. A Kruskal-Wallis test was performed, followed by Wilcoxon rank-sum tests and Bonferroni adjustment for multiple comparisons. **** $p_{adj} < 0.0001$. (C-E) The number of individuals affected and the total number of people surveyed is tallied at the end of each bar. (C) Simons Searchlight data documenting the percentage of affected individuals (teal bars) and their unaffected family members (gray bars) who reported GI issues in caregiver surveys. (D) Ciitizen® medical record data showing the percentage of individuals with a *SYNGAP1*, *SCN2A*, *CHD2*, *STXBP1* or *SLC6A1* genetic variant with medical record diagnoses related to GI dysmotility. (E) Ciitizen® medical record data by variant for dysmotility phenotypes including constipation, abdominal pain, and diarrhea.

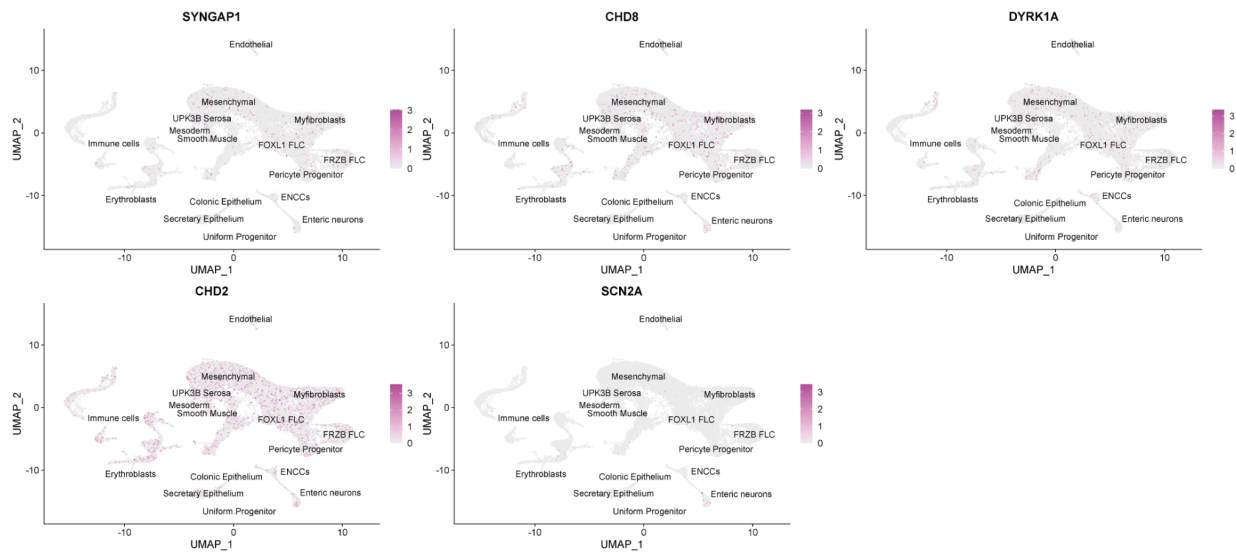


Figure 3.3. hcASD gene expression in human prenatal gut transcriptomic dataset¹¹⁶.

UMAPs of *SYNGAP1*, *CHD8*, *SCN2A*, *CHD2*, and *DYRK1A* expression.

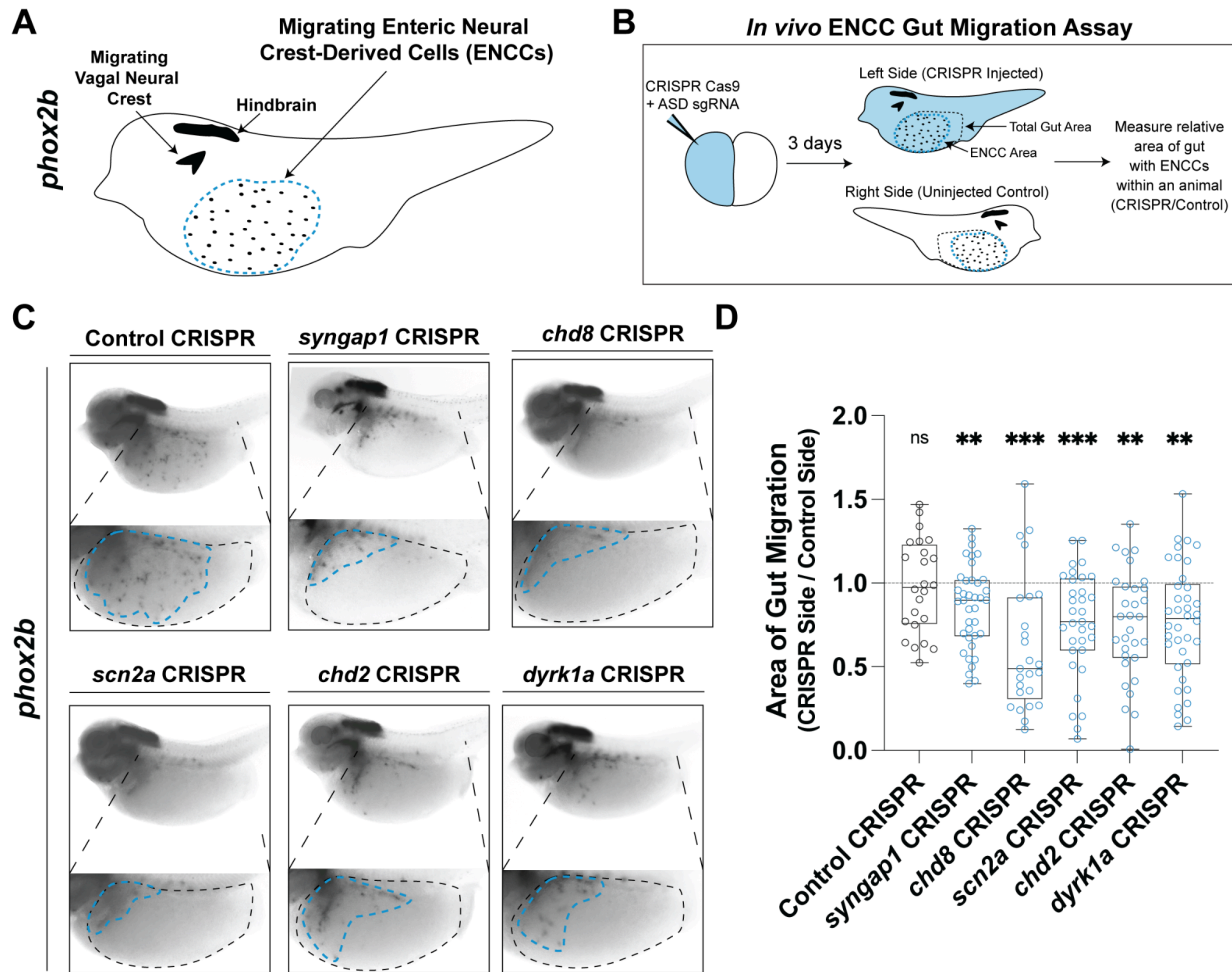


Figure 3.4. hcASD gene depletion *in vivo* causes ENCC migration defects.

(A) Schematic of *phox2b* staining in NF stage 40 animals to mark enteric neural crest-derived cells (ENCCs, enteric neuron progenitors) in the gut, circled by a blue dashed line. *phox2b* also labels the hindbrain region and other migrating vagal neural crest cells. (B) Unilateral mutants were made by injecting the Cas9 protein and an sgRNA targeting an hcASD gene into one cell at the two-cell embryonic stage. Three days later, injected embryos were stained and ENCC area and gut area was measured on each side of the animal and compared to quantify relative gut area (CRISPR side / Control side) of migration. (C) Individual CRISPR mutagenesis of hcASD genes *syngap1*, *chd8*, *scn2a*, *chd2*, or *dyrk1a* reduce the area of ENCC migration in the gut compared to control mutagenesis of pigmentation gene *slc45a2*. (D) Area of gut migration quantification by target gene. Control in gray, hcASD genes in blue. A Kruskal-Wallis test was performed followed by Wilcoxon matched-pairs signed rank test to compare the CRISPR side to the control side within each animal and a Holm-Šídák test to adjust for multiple comparisons. ns (not significant) indicates $p_{adj} > 0.05$, ** $p_{adj} < 0.01$, *** $p_{adj} < 0.001$.

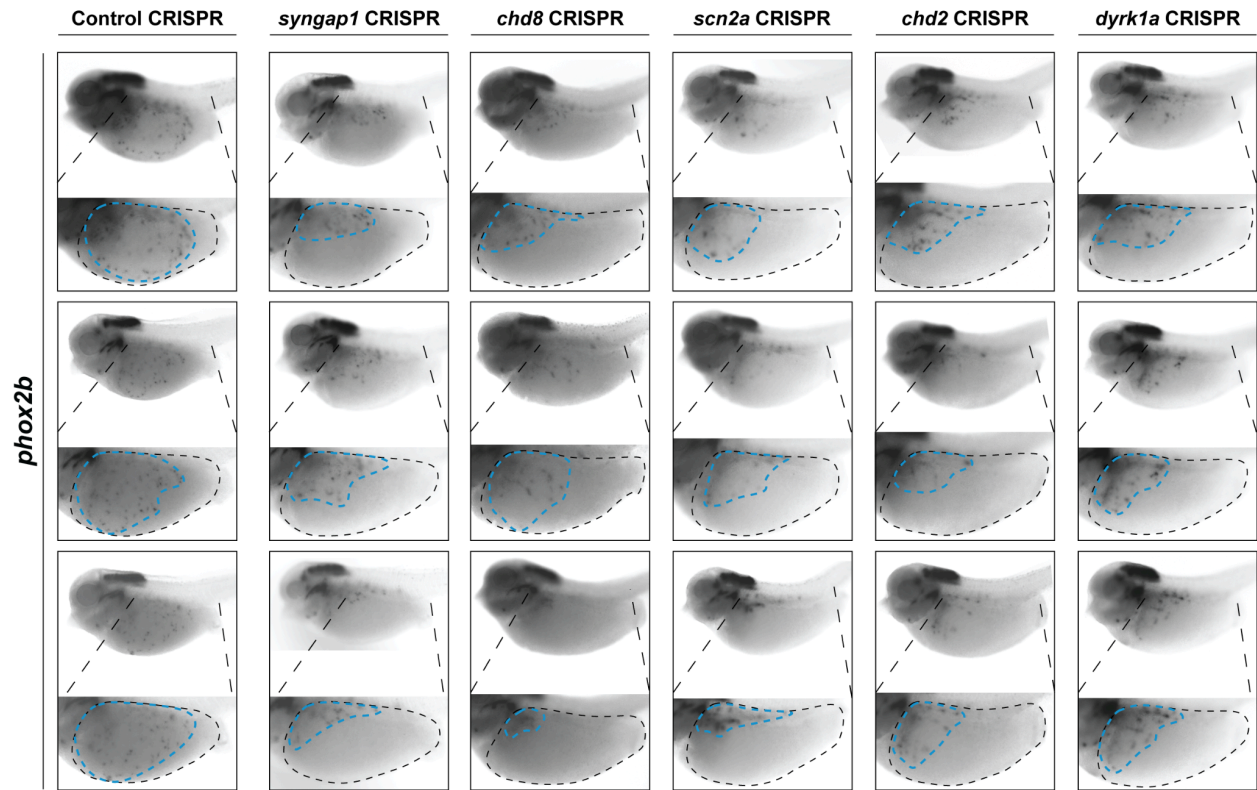


Figure 3.5. Additional representative images of hcASD gene knockdowns. CRISPR mutagenesis of hcASD genes *syngap1*, *chd8*, *scn2a*, *chd2*, or *dyrk1a* show reduced area of ENCC migration but with no consistent migratory patterns between genes.

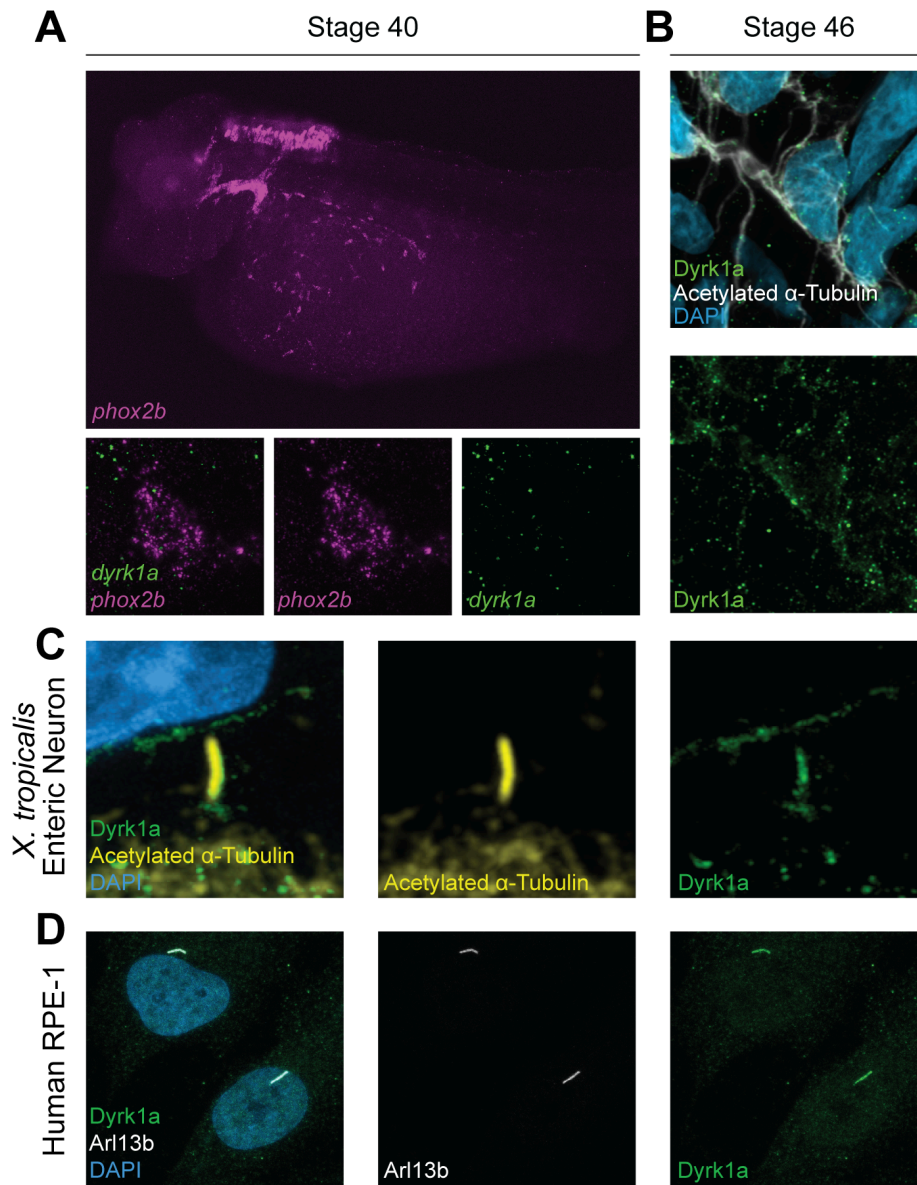


Figure 3.6. *dyrk1a* is expressed in ENCCs and Dyrk1a localizes to microtubule-based structures.

(A) RNA *in situ* hybridization chain reaction staining shows *dyrk1a* (green) expression in *phox2b*-positive (magenta) ENCCs in *X. tropicalis*, stage 40. Bottom panel shows a high magnification image of *dyrk1a* mRNA transcripts within a single *phox2b*-positive cell. (B) Immunofluorescence staining shows Dyrk1a (green) localizing to enteric neuron projections in *X. tropicalis* as marked by Acetylated α -Tubulin (white). (C) Immunofluorescence staining shows Dyrk1a (green) localizing to the primary cilium of an enteric neuron in *X. tropicalis* as marked by Acetylated α -Tubulin (yellow). (D) Immunofluorescence staining shows localization of Dyrk1a (green) to the primary cilium of human retinal pigmented epithelial (RPE-1) cells as marked by Arl13b antibody staining (white).

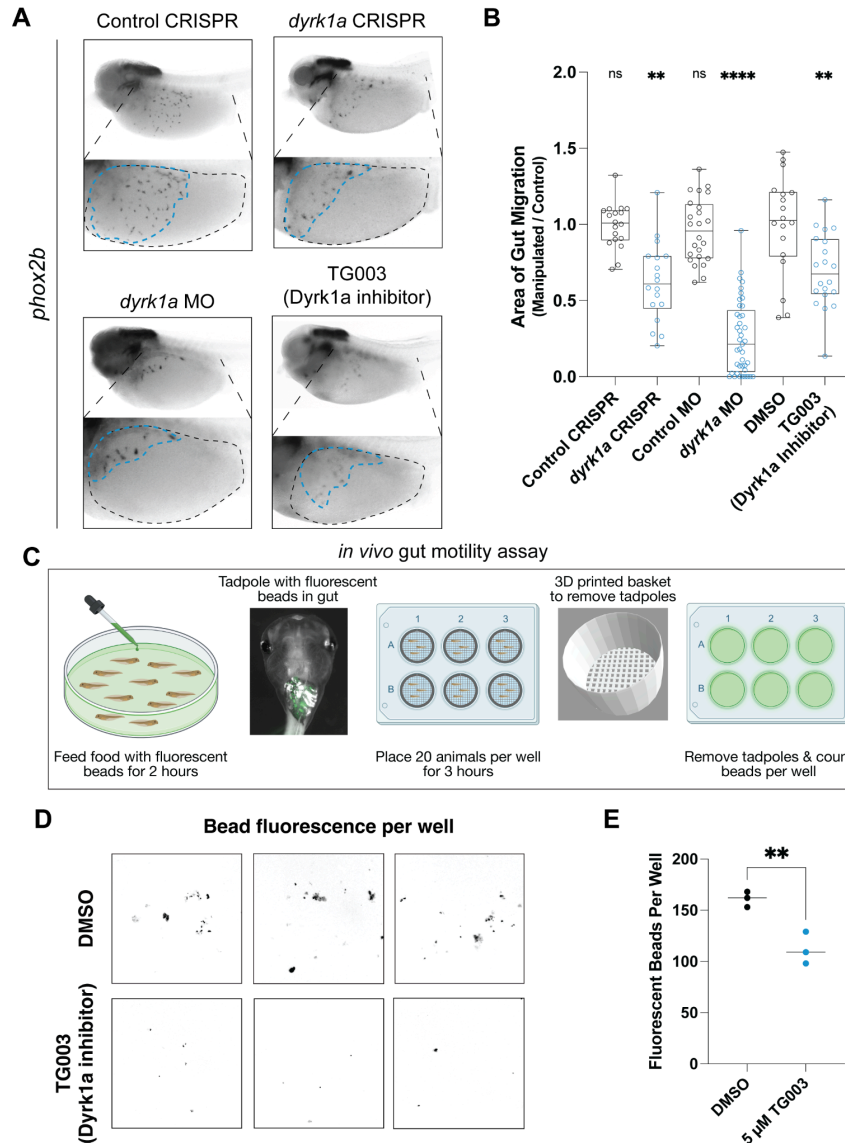


Figure 3.7. hcASD gene *dyrk1a* perturbation reduces ENCC migration and decreases gut motility *in vivo*.

(A) *dyrk1a* perturbation through CRISPR injection, morpholino (MO) injection, or Dyrk1a inhibitor (TG003) treatment all reduce the area of ENCC migration in the gut compared to control CRISPR, control MO, or vehicle control (DMSO). (B) Area of gut migration quantification by condition. For injection comparisons, a Two-Way ANOVA was performed followed by Wilcoxon matched-pairs signed rank test to compare the CRISPR or morpholino side to the control side within each animal and a Holm-Šídák test to adjust for multiple comparisons. p values are from paired t tests, in which ns (not significant) indicates $p_{adj} > 0.05$, *dyrk1a* CRISPR $p_{adj} = 0.0094$, *dyrk1a* MO $p_{adj} < 0.0001$. For small molecule treatment, an unpaired student's one-tailed t-test was performed after testing for normality to compare DMSO to 5 μ M TG003-treated embryos. TG003 $p = 0.0012$. (Figure caption continued on the next page.)

(Figure caption continued from the previous page.) (C) Schematic of the *in vivo* gut motility assay. At NF stage 47, tadpoles were fed food with fluorescent beads for 2 hours, then placed in a 6-well plate in 3D-printed baskets with 20 animals/well for 3 hours. Tadpoles are then removed by taking out baskets and leaving excrement with fluorescent beads behind, after which the plates were imaged to count the number of beads per well. Created with BioRender.com. (D) Developmental inhibition of Dyrk1a (TG003-treated beginning at NF 20) results in decreased fluorescent bead excretion compared to vehicle control (DMSO). Representative images of fluorescent beads (false-colored black). (E) Number of fluorescent beads per well counted for DMSO and TG003 (Dyrk1a inhibitor) wells. Wilcoxon rank-sum test, $p = 0.002$.

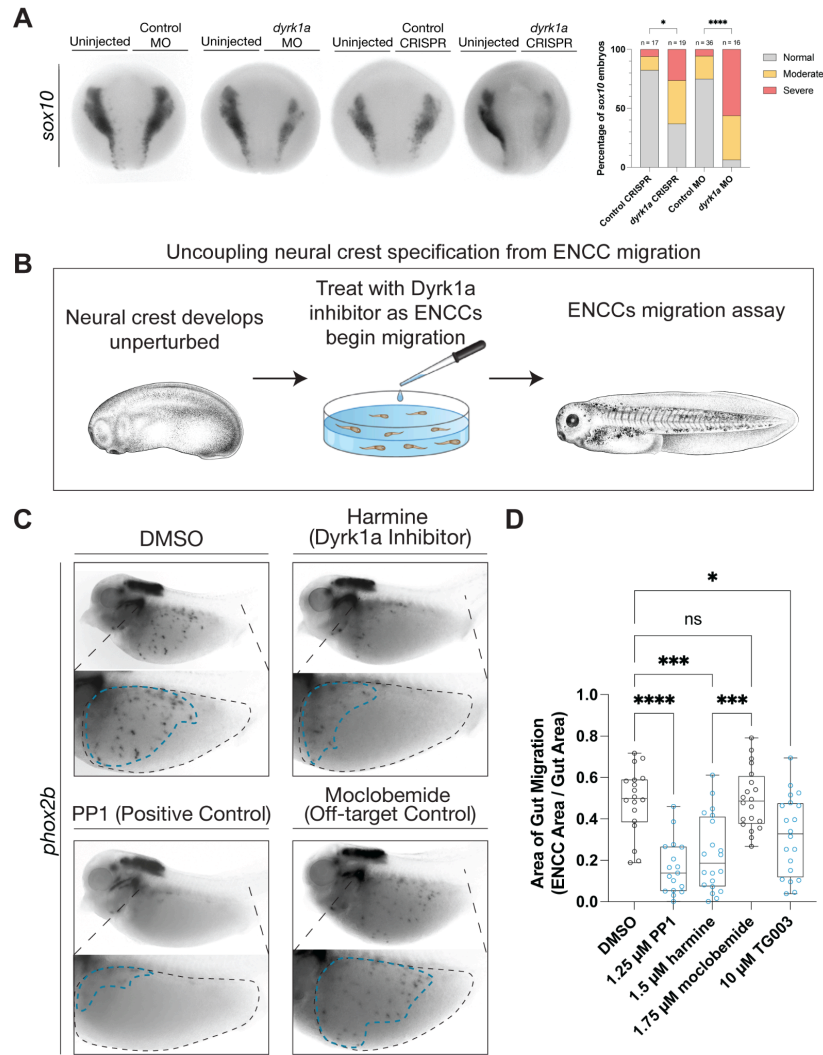


Figure 3.8. *dyrk1a* is independently required for early neural crest development and for later ENCC migration.

(A) Perturbation of *dyrk1a* with either CRISPR or morpholino (MO) injection results in an increased proportion of moderate and severe early (stage 15) neural crest phenotypes compared to controls. Migratory neural crest was visualized with RNA *in situ* hybridization staining for *sox10* at NF stage 15. There are significantly more moderate and severe phenotypes in *dyrk1a* CRISPR and MO embryos than controls (Fisher's exact test, CRISPR $p = 0.02$, MO $p < 0.0001$). (B) Schematic of assay to uncouple early neural crest development disruption from later ENCC migration. Tadpoles are raised unperturbed until NF stage 25 when the vagal neural crest begins migration. They are then treated with a Dyrk1a inhibitor or control small molecule and fixed and stained at NF stage 40 to assay ENCC migration. *Xenopus* illustrations © Natalya Zahn (2022)¹³⁸. Created with BioRender.com. (C) Treatment with Dyrk1a inhibitors harmine or TG003 as well as positive control Ret inhibitor PP1 lead to reduced ENCC migration separately from neural crest specification, compared to DMSO and moclobemide controls. (Figure caption continued on the next page.)

(Figure caption continued from the previous page.) Moclobemide is a monoamine oxidase inhibitor that controls for potential off-target inhibition of monoamine oxidase by harmine. (D) Area of gut migration quantification by condition. Controls in gray, Dyrk1a inhibitors in blue. A One-Way ANOVA was performed followed by a Holm-Šídák test to adjust for multiple comparisons. p values are from paired t tests, in which ns (not significant) indicates $p_{adj} > 0.05$. Compared to DMSO, PP1 $p_{adj} < 0.0001$, harmine $p_{adj} < 0.0001$, TG003 $p_{adj} = 0.0046$, and compared to moclobemide, harmine $p_{adj} < 0.0001$.

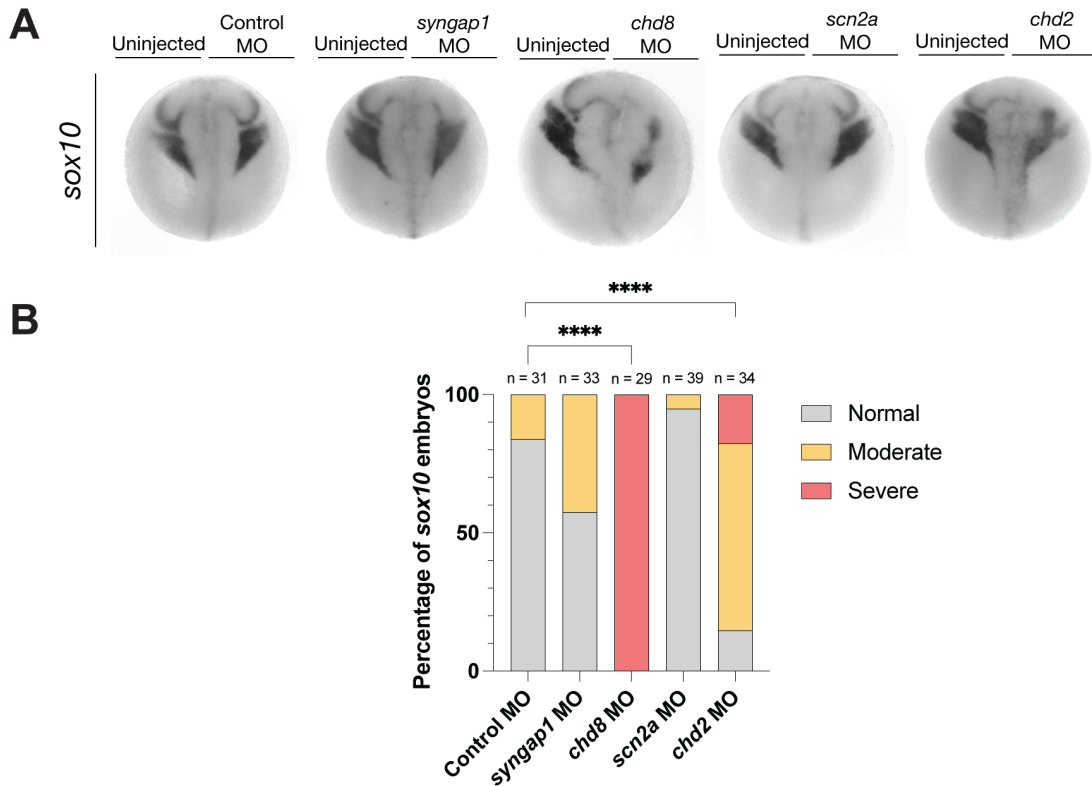


Figure 3.9. hcASD genes *chd8* and *chd2* are required for neural crest development.

(A) Perturbation of hcASD genes *syngap1*, *chd8*, *scn2a* or *chd2* in early (NF stage 20) embryos. (B) Proportion of severe, moderate, and normal embryo quantification by target gene. A Fisher's exact test was performed to compare the proportions to the control condition, and p-values were corrected for multiple comparisons. ****p < 0.0001. There is an increased proportion of moderate and severe neural crest phenotypes in *chd8* and *chd2* conditions compared to controls. There is a slight increase in the proportion of moderate phenotypes in *syngap1* embryos (p-value = 0.02 before multiple comparisons correction) and no effect on *scn2a* embryos compared to controls.

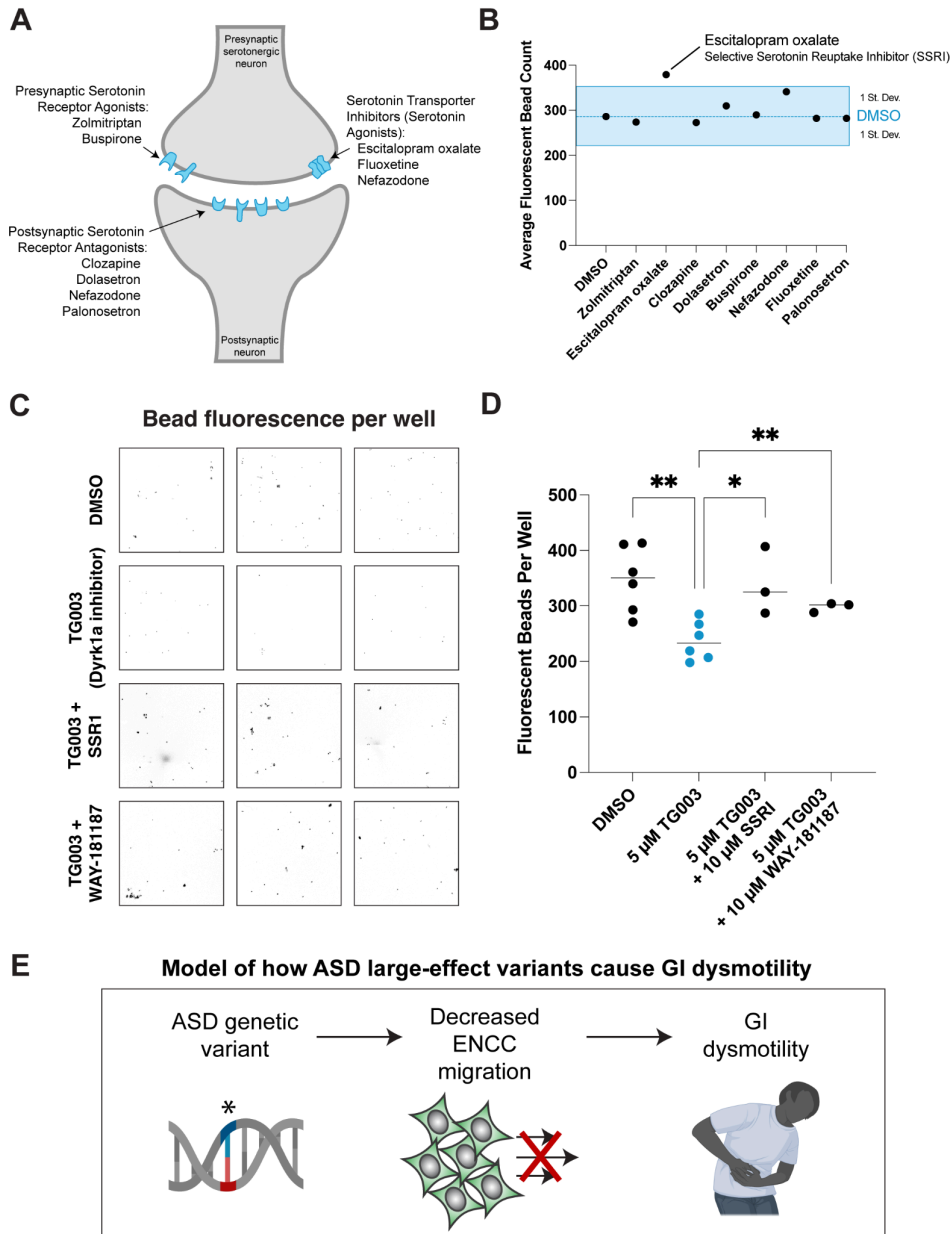


Figure 3.10. Dyrk1a-associated gut dysmotility is ameliorated by acute exposure to an SSRI or 5-HTR6 agonist.

(A) Schematic of a serotonergic synapse labeling the presumed location of action for the drugs tested. (B) Acute exposure to escitalopram oxalate (selective serotonin reuptake inhibitor, SSRI) alone increases the average number of fluorescent beads excreted by more than one standard deviation compared to the average DMSO treatment, blue. (C) Both acute treatment of an SSRI (10 μ M escitalopram oxalate) or a 5HTR6 agonist (10 μ M WAY-181187) rescue the decreased fluorescent bead excretion from developmentally inhibited Dyrk1a (5 μ M TG003 starting at stage NF 20) animals. (D) Fluorescent beads per well quantified for each treatment condition. (Figure caption continued on the next page.)

(Figure caption continued from the previous page.) A one-way ANOVA was performed followed by unpaired one-tailed t tests with welch's correction compared to TG003 treatment, DMSO $p = 0.002$, TG003 + SSRI $p = 0.0423$, TG003 + WAY-181187 $p = 0.0033$. (E) Model of how hcASD gene large-effect variants could contribute to GI dysmotility. An hcASD genetic variant leads to perturbed ENCC migration and ultimately GI dysmotility. Created with BioRender.com.

Table 3.1. Summary table of patient GI symptoms from Ciitizen® records for individuals with variants in *SYNGAP1*. Individuals with *SYNGAP1* variants display high rates of GI dysmotility.

SYNGAP1	Counts	Percentage
Number of Patients	186	100
Any GI	168	90.3225806
Any Dysmotility	136	73.1182796
Any Constipation	117	62.9032258
Any Vomiting	41	22.0430108
Any Diarrhea	25	13.4408602
Any Reflux	52	27.9569892
Constipation	83	44.6236559
Vomiting	40	21.5053763
Chronic constipation	34	18.2795699
Diarrhea	23	12.3655914
Abdominal pain	20	10.7526882
Incontinence of feces	13	6.98924731
Encopresis	8	4.30107527
Nausea	5	2.68817204
Bowel obstruction	2	1.07526882
Chronic diarrhea	2	1.07526882
Altered bowel function	1	0.53763441
Bilious vomiting	1	0.53763441
Gastrointestinal dysmotility	1	0.53763441
Gastroparesis	1	0.53763441
Projectile vomiting	1	0.53763441
Uncontrollable vomiting	1	0.53763441

Table 3.2. Summary table of patient GI symptoms from Ciitizen® records for individuals with variants in SCN2A. Individuals with SCN2A variants display high rates of GI dysmotility.

SCN2A	Counts	Percentage
Number of Patients	58	100
Any GI	55	94.8275862
Any Dysmotility	47	81.0344828
Any Constipation	41	70.6896552
Any Vomiting	24	41.3793103
Any Diarrhea	16	27.5862069
Any Reflux	36	62.0689655
Constipation	29	50
Vomiting	23	39.6551724
Abdominal pain	18	31.0344828
Diarrhea	15	25.862069
Chronic constipation	12	20.6896552
Incontinence of feces	8	13.7931034
Gastrointestinal dysmotility	7	12.0689655
Nausea	3	5.17241379
Bowel obstruction	2	3.44827586
Encopresis	2	3.44827586
Bilious vomiting	1	1.72413793
Chronic diarrhea	1	1.72413793
Cyclical vomiting syndrome	1	1.72413793
Gastroparesis	1	1.72413793
Projectile vomiting	1	1.72413793
Severe diarrhea	1	1.72413793

Table 3.3. Summary table of patient GI symptoms from Ciitizen® records for individuals with variants in *CHD2*. Individuals with *CHD2* variants display high rates of GI dysmotility.

CHD2	Counts	Percentage
Number of Patients	41	100
Any GI	35	85.3658537
Any Dysmotility	27	65.8536585
Any Constipation	20	48.7804878
Any Vomiting	10	24.3902439
Any Diarrhea	3	7.31707317
Any Reflux	13	31.7073171
Constipation	11	26.8292683
Chronic constipation	10	24.3902439
Vomiting	10	24.3902439
Abdominal pain	4	9.75609756
Diarrhea	2	4.87804878
Chronic diarrhea	1	2.43902439
Gastroparesis	1	2.43902439
Nausea	1	2.43902439

Table 3.4. Summary table of patient GI symptoms from Ciitizen® records for individuals with variants in *STXBP1*. Individuals with *STXBP1* variants display high rates of GI dysmotility.

STXBP1	Counts	Percentage
Number of Patients	80	100
Any GI	64	80
Any Dysmotility	48	60
Any Constipation	37	46.25
Any Vomiting	21	26.25
Any Diarrhea	11	13.75
Any Reflux	30	37.5
Constipation	32	40
Vomiting	21	26.25
Diarrhea	10	12.5
Incontinence of feces	7	8.75
Abdominal pain	6	7.5
Chronic constipation	5	6.25
Gastrointestinal dysmotility	2	2.5
Nausea	2	2.5
Chronic diarrhea	1	1.25
Cyclical vomiting syndrome	1	1.25
Encopresis	1	1.25
Gastroparesis	1	1.25
Projectile vomiting	1	1.25

Table 3.5. Summary table of patient GI symptoms from Ciitizen® records for individuals with variants in *SLC6A1*. Individuals with *SLC6A1* variants display high rates of GI dysmotility.

SLC6A1	Counts	Percentage
Number of Patients	49	100
Any GI	42	85.7142857
Any Dysmotility	35	71.4285714
Any Constipation	29	59.1836735
Any Vomiting	11	22.4489796
Any Diarrhea	6	12.244898
Any Reflux	15	30.6122449
Constipation	23	46.9387755
Vomiting	10	20.4081633
Chronic constipation	6	12.244898
Abdominal pain	5	10.2040816
Chronic diarrhea	3	6.12244898
Diarrhea	3	6.12244898
Encopresis	3	6.12244898
Nausea	2	4.08163265
Projectile vomiting	2	4.08163265

Materials and Methods

Simons Searchlight and Ciitizen® Patient Data Analysis

Research with Simons Foundation Autism Research Initiative (SFARI) Simons Collection (Searchlight) data and with Ciitizen® medical record data was determined to be non-human subjects research by UCSF IRB office, IRB#23-39-079. Unaffected family and affected individual GI data was accessed through the Simons Searchlight Single Gene Dataset v8.0. All data was used from families with any genetic variant in a hcASD gene, as defined by Fu et al. 2022³¹ with an FDR < 0.1. Patient GI data was additionally accessed from Ciitizen®. Patients were included if they possessed a genetic variant that was classified on their genetic report as 'pathogenic', 'likely pathogenic', or 'variant of uncertain significance'. Individuals with 'benign' variants in a hcASD gene were excluded. Individuals with a 'variant of uncertain significance' in a hcASD gene in addition to a 'pathogenic' variant in a non-ASD gene were also excluded. Data analysis and visualization were performed in Prism (v.10.1.1) software.

Human prenatal intestine scRNA-sequencing analysis and enrichment scoring

First, scRNA-seq FASTQ files of human prenatal intestine (ArrayExpress: E-MTAB-9489¹¹⁶) were downloaded from ArrayExpress and processed by Cell Ranger (GRCh38). Following the standard Seurat analysis pipeline, we read the gene-barcode matrix outputs of all samples and filtered out low quality cells that had > 10% mitochondrial counts and unique feature counts over 2,500 or less than 200, leaving 39,095 cells. Normalization was then done with the gene-barcode matrix with method

LogNormalize that normalized each cell by total expression and multiplied by the default scale factor (10,000).

2,000 highly variable genes of each sample were identified with function FindVariableFeatures then all samples were integrated with method IntegrateData to form a combined Seurat object for downstream analysis. Integrated object was then scaled and Principal Component Analysis was performed for dimensional reduction. FindNeighbors and FindClusters were used to compute cell clusters of the object. Next, identification of cell clusters was performed using gene markers from Elmentaite et al. 2020¹³⁹ in addition to ENCC markers (*SOX10*, *FOXD3*, *PHOX2B*) and enteric neuron markers (*TUBB3*, *ELAVL4*, *RET*) to finalize cell annotations.

To assess enrichment of hcASD genes, AddModuleScore function was performed for the 252 hcASD genes from Fu et al. 2022 and compared against a control geneset with equivalent average expression across all cells. Each cell received a module score and was then grouped based on cell annotation as described above. A cell expressing hcASD genes higher than the control geneset received a score > 0 , while a cell expressing the control geneset higher than the hcASD genes had a score of < 0 . Cells were then grouped into Non-ENS cells, ENCCs, and enteric neurons based on the above clustering. Next we tested whether ENCCs and enteric neurons had significantly higher hcASD gene expression enrichment scores, compared to all other cells by a Kruskal-Wallis test, followed by Wilcoxon rank-sum tests and Benjamini-Hochberg adjustment for multiple comparisons. The enrichment of these genes in each cluster or group was plotted using VlnPlot.

***Xenopus* husbandry**

Xenopus laevis or *tropicalis* adults originated from the National Xenopus Resource Center¹⁰¹ and the Khokha Lab. Animals used were of wildtype lines of both sexes. Animals were housed in a recirculating system and were maintained in accordance with approved UCSF IACUC protocol AN199587-00A. Ovulation was induced with human chorionic gonadotropin (Sigma CG10), and embryos were collected and manipulated according to standard procedure¹⁰². Gut motility experiments were done in *Xenopus laevis*, while migration experiments were done in *Xenopus tropicalis*. The *Xenopus* community resource Xenbase was referenced daily⁸⁷.

***Xenopus tropicalis* microinjections and loss of function**

A Narishige micromanipulator, Parker or Narishige Picospritzers, and Zeiss Stemi508 microscopes were used to microinject reagents into 1 cell of 2-cell stage embryos. For morpholino injections, 2 nl injection volume of each condition was measured using an eyepiece micrometer, delivering 2 ng of the morpholino per blastomere. Embryos were injected and grown at 20-25°C in 1/9 Modified Ringer's (MR) solution. Published and validated translation-blocking *dyrk1a* morpholino (5' TGCATCGTCCTCTTTCAAGTCTCAT 3')^{72,119} was compared against a standard control morpholino (5' CCTCTTACCTCAGTTACAATTTATA 3', GeneTools). For the supplemental *sox10* experiment (**Fig. S5**), translation-blocking morpholinos for *syngap1* (5.5 ng, 5' GAGCATAGAACATCATTCCACAGCT 3', GeneTools), *chd8* (3.2 ng, 5' CCAGCCTGTGAGAGAAGATAGTAAT 3', GeneTools), *scn2a* (3.2 ng, 5' ATTCTGGAGGATTACTCAAGGTCAT 3', GeneTools), and *chd2* (3.2 ng, 5'

GGTTTATCCTCATTCCCTCATCATTG 3')¹⁴⁰ were compared against 5.5 ng of the standard control morpholino.

For CRISPR, we synthesized (EnGen, NEB E3322S) and purified (Zymo R1018) validated sgRNAs⁷¹ and injected 400 pg of sgRNA and 2.24 ng of Cas9-NLS protein (UC Berkeley MacroLabs¹⁴¹) into 1 cell of 2-cell stage *X. tropicalis* embryos. The exceptions to this are *syngap1* and corresponding *slc45a2* control where embryos were injected with 800 pg of sgRNA and 4.48 ng of Cas9-NLS protein, since the *syngap1* sgRNA is of lower mutational efficiency. Injection volume was measured using an eyepiece micrometer and embryos were incubated at 27°C for 1 hour immediately after injection and then grown at 20-25°C in 1/9 MR solution.

***Xenopus* whole-mount RNA *in situ* hybridization**

All embryos were fixed in MEMFA for 1 hour and stained according to Willsey et al 2021¹⁰³ using anti-DIG (1:3000, Sigma 11093274910) and BM Purple (Sigma 11442074001). *phox2b* probe plasmid was a kind gift from the Harland lab (IMAGE clone #8956276, probe synthesis with T7 enzyme and EcoR1 restriction enzyme), and *sox10* probe was previously described⁷¹. The stainings were performed in a high-throughput basket format with 200 µm mesh in 3D-printed racks^{103,104}. All embryos were imaged on a Zeiss AxioZoom.V16 with a 1x objective and extended depth of focus processing in Zeiss Zen software.

For hybridization chain reaction (HCR)¹⁴², embryos were stained according to Willsey et al 2021¹⁰³, with an additional step of heating probes to 95°C for 90 seconds and cooling to room temperature before use. *dyrk1a* and *phox2b* probes were custom ordered

through Molecular Instruments and designed to target the *X. tropicalis* genes. Embryos were imaged on a Zeiss 980 LSM with a 63x oil objective, Airyscan processed and Maximum Intensity Projection performed in Zen or on a Zeiss AxioZoom.V16 with a 1x objective and extended depth of focus for full-embryo imaging.

Drug treatment

Dyrk1a inhibitor (TG003, Sigma T5575) and MAO inhibitor control (Moclobemide, Sigma M3071) were resuspended in DMSO at 10 mM. Dyrk1a inhibitor (harmine, Sigma 286044) and Ret inhibitor (PP1, Sigma P0040) were resuspended in DMSO at 1 mM. Embryos were treated with drug or an equal volume of DMSO, diluted in 1/9 MR, at NF stage 25 and fixed at NF stage 40 for RNA *in situ* hybridization staining. Media was not refreshed while embryos were growing. For the serotonin gut motility screen (see below), selected drugs from an FDA-approved drug library (Enzo Life Sciences BML-2843-0100) were tested at 10 μ M alongside an equal volume of DMSO diluted in 1/3 MR.

Gut motility assay

All gut motility assays were performed in *Xenopus laevis*, since pilot studies showed they excrete more than *X. tropicalis* (they are larger animals), which was enough to be able to reliably quantify bead number per well from 20 animals. Since these experiments are all drug treatments and not genetic perturbations, the advantages of the *X. tropicalis* diploid genome are less critical. *Xenopus laevis* embryos were collected and raised for 9 days at room temperature until NF stage 47. At the beginning of the gut motility assay, tadpoles were moved into 15 cm dishes containing 20 mL of 1/3 MR.

Food was prepared by resuspending 1 g of sera micron (Sera 00720) in 45 mL of 1/3 MR with 30 μ L of 6 μ m fluorescent bead solution (Polysciences 18862-1) added, similarly to what has previously been used to assay gut motility in zebrafish³⁷. 2.5 mL of the food suspension was added to each 15 cm dish for each condition. Tadpoles were left to feed for 2 hours and then rinsed in a homemade mesh (Spectra Mesh 100 μ m and 200 μ m, 146488 and 146487) trough in a glass dish (Grainger 900203). Using a vacuum, media was removed while fresh 1/3 MR was added until the media was clear of food and beads. Tadpoles were moved from the mesh trough using a plastic pipette into a fresh 15 cm dish. They were then transferred to a 6-well plate with homemade 3D-printed baskets with lattice bottoms inserted into each well. 20 tadpoles were allotted into each basket. After defecating for 3 hours, baskets with tadpoles were removed from each well, leaving excretion with fluorescent beads in the well. All plates were left in the dark at 4°C overnight to let all matter sink to the bottom of the plate. Then, plates were tile-imaged in the same position on a Zeiss AxioZoom.V16 with a 1x objective and analyzed in Fiji.

When raising animals in Dyrk1a inhibitor, TG003 or equivalent volume of DMSO was added to 1/3 MR to make it a 5 μ M TG003 solution. 75 NF stage 20 *X. laevis* embryos were treated for each condition. For the serotonin screen, tadpoles were raised only in 1/3 MR until the 3-hour defecation period, at which point they were acutely exposed to 10 μ M of each compound individually. For the rescues, animals were grown in DMSO or 5 μ M TG003 starting at stage 20. At stage 47, animals were removed from drug solution and fed beads in 1/3 MR as above. Following feeding, animals were left to defecate either in 1/3 MR or in 10 μ M SSRI or 5-HTR6 drug solution in 1/3MR.

Image Processing and Statistical Analyses

All images were processed in FIJI (NIH) and arranged in Illustrator (Adobe). For ENCC quantification, the area of ENCCs and total gut area were both measured by drawing with the free-hand selection tool and quantified with the measure function. The ENCC area was normalized to the total gut area. Tests for normality were performed in Prism (GraphPad) followed by an ANOVA or Kruskal-Wallis test as appropriate. For unilateral mutagenesis, multiple paired t tests were performed to compare the uninjected and injected sides of each embryo per condition and then adjusted for multiple comparisons with the Holm-Šídák method. For small molecule experiments, a one-way ANOVA or Kruskal-Wallis test was used as appropriate based on normality tests, followed by an unpaired t test or a Wilcoxon rank-sum test.

For gut motility image analysis, tiled images were analyzed in FIJI with a macro to Find Maxima (Prominence > 60, Output type: Count) in each well of a 6-well plate. Counts were imported into Prism and standard deviation was calculated for control treatments. For comparing between DMSO, TG003 and rescue treatments, all conditions passed normality and a one-way ANOVA was performed followed by unpaired one-tailed t tests with Welch's correction.

Cell culture

84,000 RPE-1-hTERT (ATCC CRL-4000) cells per well were seeded into 24-well Corning cell culture dishes in DMEM F12 (Thermo Fisher Catalog # 11320-082) supplemented with 10% Fetal Bovine Serum, incubated at 37°C, in 5% CO₂ for 24 hours. After 24 hours, cell media was replaced with reduced serum media OptiMEM (Thermofisher 31985062) to induce serum starvation. 24 hours later, cells were fixed

with 4% PFA for 10 minutes, washed with three times PBS, and stored at 4°C for further processing.

Immunofluorescence staining

For NF stage 45 samples, Immunostaining was performed according to Willsey et al 2021¹⁰³ with the omission of the bleaching step as it was found to add bubbles that affected GI morphology. Phalloidin (1:400, Life Tech A34055) and DAPI (1:400) were added during the secondary antibody step. Primary antibodies used were against Dyrk1a (1:100, R&D Systems AF5407) or Acetylated α -Tubulin (1:200, Abcam ab179484). Secondary antibodies (Abcam ab150177, ThermoFisher A32733) were diluted at 1:250. Embryos were imaged on a Zeiss 980 LSM with a 63x oil objective, Airyscan processing and Maximum Intensity Projection were performed in Zen.

RPE-1 cells were permeabilized with PBST (1X PBS at pH 7.4 containing 0.2% Triton X-100) three times for 5 minutes and blocked with 2% BSA (Sigma-Aldrich A70906 in PBST) for 5 hours at room temperature. Primary antibodies were diluted into 2% BSA and cells were incubated at 4°C overnight. Antibodies used were ARL13B (1:2000, ProteinTech 17711-1-AP) and Dyrk1a (1:250, R&D Systems AF5407). Following primary antibody incubation, cells were washed three times for 5 minutes in PBST, protected from light. Secondary antibodies (Thermo A32732 or Thermo A32728) were diluted at 1:1000 in 2% BSA, and DAPI was included in this secondary incubation at 1:1000. Cells were incubated in diluted secondary antibodies for 1 hour at room temperature, protected from light. Stained cells were washed with PBST three times for 5 minutes and with 1X PBS two times; cells were stored at 4°C. Cells were imaged on a Zeiss 980 LSM with a 63x oil objective. Maximum intensity projection was performed in FIJI.

References

1. Furness, J. B. & Stebbing, M. J. The first brain: Species comparisons and evolutionary implications for the enteric and central nervous systems. *Neurogastroenterol Motil* **30**, (2018).
2. Rao, M. & Gershon, M. D. Enteric nervous system development: what could possibly go wrong? *Nat Rev Neurosci* **19**, 552–565 (2018).
3. Avetisyan, M., Schill, E. M. & Heuckeroth, R. O. Building a second brain in the bowel. *J. Clin. Invest.* **125**, 899–907 (2015).
4. Niesler, B., Kuerten, S., Demir, I. E. & Schäfer, K.-H. Disorders of the enteric nervous system — a holistic view. *Nature Reviews Gastroenterology & Hepatology* **18**, 393–410 (2021).
5. Lake, J. I. & Heuckeroth, R. O. Enteric nervous system development: migration, differentiation, and disease. *Am. J. Physiol. Gastrointest. Liver Physiol.* **305**, G1–24 (2013).
6. Medina-Cuadra, L. & Monsoro-Burq, A. H. Xenopus, an emerging model for studying pathologies of the neural crest. *Curr Top Dev Biol* **145**, 313–348 (2021).
7. Simkin, J. E., Zhang, D., Rollo, B. N. & Newgreen, D. F. Retinoic acid upregulates ret and induces chain migration and population expansion in vagal neural crest cells to colonise the embryonic gut. *PLoS One* **8**, e64077 (2013).
8. Young, H. M. *et al.* Colonizing while migrating: how do individual enteric neural crest cells behave? *BMC Biology* **12**, 1–18 (2014).
9. Drokhlyansky, E. *et al.* The Human and Mouse Enteric Nervous System at Single-Cell Resolution. *Cell* **182**, 1606–1622.e23 (2020).

10. Costa, M., Brookes, S. J. & Hennig, G. W. Anatomy and physiology of the enteric nervous system. *Gut* **47 Suppl 4**, iv15–9; discussion iv26 (2000).
11. Bornstein, J. C., Costa, M. & Grider, J. R. Enteric motor and interneuronal circuits controlling motility. *Neurogastroenterol Motil* **16 Suppl 1**, 34–38 (2004).
12. Amiel, J. & Lyonnet, S. Hirschsprung disease, associated syndromes, and genetics: a review. *Journal of Medical Genetics* **38**, 729–739 (2001).
13. Bergeron, K.-F., Silversides, D. W. & Pilon, N. The developmental genetics of Hirschsprung's disease. *Clinical Genetics* **83**, 15–22 (2013).
14. Vaezi, M. F. *et al.* Achalasia: from diagnosis to management. *Ann N Y Acad Sci* **1381**, 34–44 (2016).
15. Furuzawa-Carballeda, J. *et al.* New insights into the pathophysiology of achalasia and implications for future treatment. *World J. Gastroenterol.* **22**, 7892–7907 (2016).
16. Richter, J. E. The diagnosis and misdiagnosis of Achalasia: it does not have to be so difficult. *Clin Gastroenterol Hepatol* **9**, 1010–1011 (2011).
17. Swanström, L. L. Achalasia: treatment, current status and future advances. *Korean J Intern Med* **34**, 1173–1180 (2019).
18. Jia, X. *et al.* Achalasia: The Current Clinical Dilemma and Possible Pathogenesis. *J Neurogastroenterol Motil* **29**, 145–155 (2023).
19. McElhanon, B. O., McCracken, C., Karpen, S. & Sharp, W. G. Gastrointestinal symptoms in autism spectrum disorder: a meta-analysis. *Pediatrics* **133**, 872–883 (2014).
20. Wang, X. *et al.* The enteric nervous system deficits in autism spectrum disorder.

- Front. Neurosci.* **17**, 1101071 (2023).
21. Wasilewska, J. & Klukowski, M. Gastrointestinal symptoms and autism spectrum disorder: links and risks – a possible new overlap syndrome. *Pediatric Health, Medicine and Therapeutics* **6**, 153–166 (2015).
 22. Hughes, M. M. *et al.* The Prevalence and Characteristics of Children With Profound Autism, 15 Sites, United States, 2000-2016. *Public Health Rep.* **138**, 971–980 (2023).
 23. Hung, L. Y. & Margolis, K. G. Autism spectrum disorders and the gastrointestinal tract: insights into mechanisms and clinical relevance. *Nat Rev Gastroenterol Hepatol* **21**, 142–163 (2024).
 24. Niesler, B. & Rappold, G. A. Emerging evidence for gene mutations driving both brain and gut dysfunction in autism spectrum disorder. *Mol. Psychiatry* **26**, 1442–1444 (2021).
 25. Sotelo-Orozco, J. & Hertz-Picciotto, I. The Association Between Gastrointestinal Issues and Psychometric Scores in Children with Autism Spectrum Disorder, Developmental Delays, Down Syndrome, and Typical Development. *Journal of Autism and Developmental Disorders* 1–11 (2024).
 26. Fattorusso, A., Di Genova, L., Dell’Isola, G. B., Mencaroni, E. & Esposito, S. Autism Spectrum Disorders and the Gut Microbiota. *Nutrients* **11**, (2019).
 27. Finegold, S. M. *et al.* Pyrosequencing study of fecal microflora of autistic and control children. *Anaerobe* **16**, 444–453 (2010).
 28. De Angelis, M. *et al.* Fecal microbiota and metabolome of children with autism and pervasive developmental disorder not otherwise specified. *PLoS One* **8**, e76993

- (2013).
29. Geng, Z.-H., Zhu, Y., Li, Q.-L., Zhao, C. & Zhou, P.-H. Enteric Nervous System: The Bridge Between the Gut Microbiota and Neurological Disorders. *Front Aging Neurosci* **14**, 810483 (2022).
 30. Satterstrom, F. K. *et al.* Large-Scale Exome Sequencing Study Implicates Both Developmental and Functional Changes in the Neurobiology of Autism. *Cell* **180**, 568–584.e23 (2020).
 31. Fu, J. M. *et al.* Rare coding variation provides insight into the genetic architecture and phenotypic context of autism. *Nat. Genet.* **54**, 1320–1331 (2022).
 32. Iossifov, I. *et al.* The contribution of de novo coding mutations to autism spectrum disorder. *Nature* **515**, 216–221 (2014).
 33. Willsey, H. R., Willsey, A. J., Wang, B. & State, M. W. Genomics, convergent neuroscience and progress in understanding autism spectrum disorder. *Nat. Rev. Neurosci.* **23**, 323–341 (2022).
 34. Puig, I. *et al.* Deletion of Pten in the mouse enteric nervous system induces ganglioneuromatosis and mimics intestinal pseudoobstruction. *J. Clin. Invest.* **119**, 3586–3596 (2009).
 35. Bernier, R. *et al.* Disruptive CHD8 mutations define a subtype of autism early in development. *Cell* **158**, 263–276 (2014).
 36. Grubišić, V., Kennedy, A. J., Sweatt, J. D. & Parpura, V. Pitt-Hopkins mouse model has altered particular gastrointestinal transits in vivo. *Autism Res.* **8**, 629–633 (2015).
 37. James, D. M. *et al.* Intestinal dysmotility in a zebrafish (*Danio rerio*)

- shank3a;shank3b mutant model of autism. *Mol. Autism* **10**, 3 (2019).
38. Fröhlich, H. *et al.* Gastrointestinal dysfunction in autism displayed by altered motility and achalasia in *Foxp1*^{+/-} mice. *Proc. Natl. Acad. Sci. U. S. A.* **116**, 22237–22245 (2019).
 39. Israelyan, N. & Margolis, K. G. Reprint of: Serotonin as a link between the gut-brain-microbiome axis in autism spectrum disorders. *Pharmacol Res* **140**, 115–120 (2019).
 40. Li, Z. *et al.* Essential roles of enteric neuronal serotonin in gastrointestinal motility and the development/survival of enteric dopaminergic neurons. *J. Neurosci.* **31**, 8998–9009 (2011).
 41. Margolis, K. G. *et al.* Serotonin transporter variant drives preventable gastrointestinal abnormalities in development and function. *J Clin Invest* **126**, 2221–2235 (2016).
 42. Marler, S. *et al.* Brief Report: Whole Blood Serotonin Levels and Gastrointestinal Symptoms in Autism Spectrum Disorder. *J Autism Dev Disord* **46**, 1124–1130 (2016).
 43. Acharekar, M. V. *et al.* A Systematic Review on the Efficacy and Safety of Selective Serotonin Reuptake Inhibitors in Gastrointestinal Motility Disorders: More Control, Less Risk. *Cureus* **14**, e27691 (2022).
 44. Ghaffari, P., Shoaie, S. & Nielsen, L. K. Irritable bowel syndrome and microbiome; Switching from conventional diagnosis and therapies to personalized interventions. *J Transl Med* **20**, 173 (2022).
 45. Yntema, C. L. & Hammond, W. S. Depletions and abnormalities in the cervical

- sympathetic system of the chick following extirpation of neural crest. *J Exp Zool* **100**, 237–263 (1945).
46. Le Douarin, N. M. & Teillet, M. A. The migration of neural crest cells to the wall of the digestive tract in avian embryo. *J Embryol Exp Morphol* **30**, 31–48 (1973).
 47. Elena de Bellard, M. & Bronner-Fraser, M. Neural crest migration methods in the chicken embryo. *Methods Mol Biol* **294**, 247–267 (2005).
 48. Hutchins, E. J. *et al.* Migration and diversification of the vagal neural crest. *Dev. Biol.* **444 Suppl 1**, S98–S109 (2018).
 49. Schonkeren, S. L. *et al.* An optimization and refinement of the whole-gut transit assay in mice. *Neurogastroenterol Motil* **35**, e14586 (2023).
 50. Kacmaz, H. *et al.* A simple automated approach to measure mouse whole gut transit. *Neurogastroenterol Motil* **33**, e13994 (2021).
 51. Field, H. A., Kelley, K. A., Martell, L., Goldstein, A. M. & Serluca, F. C. Analysis of gastrointestinal physiology using a novel intestinal transit assay in zebrafish. *Neurogastroenterol Motil* **21**, 304–312 (2009).
 52. Kuil, L. E., Chauhan, R. K., Cheng, W. W., Hofstra, R. M. W. & Alves, M. M. Zebrafish: A Model Organism for Studying Enteric Nervous System Development and Disease. *Front Cell Dev Biol* **8**, 629073 (2020).
 53. Hamnett, R. *et al.* Regional cytoarchitecture of the adult and developing mouse enteric nervous system. *Curr Biol* **32**, 4483–4492.e5 (2022).
 54. Swaminathan, M. *et al.* Video Imaging and Spatiotemporal Maps to Analyze Gastrointestinal Motility in Mice. *J Vis Exp* 53828 (2016).
 55. Hao, M. M. *et al.* Early emergence of neural activity in the developing mouse

- enteric nervous system. *J Neurosci* **31**, 15352–15361 (2011).
56. Lieschke, G. J. & Currie, P. D. Animal models of human disease: zebrafish swim into view. *Nat Rev Genet* **8**, 353–367 (2007).
 57. Wang, Z. *et al.* Morphological and molecular evidence for functional organization along the rostrocaudal axis of the adult zebrafish intestine. *BMC Genomics* **11**, 392 (2010).
 58. Taylor, J. S., Braasch, I., Frickey, T., Meyer, A. & Van de Peer, Y. Genome duplication, a trait shared by 22000 species of ray-finned fish. *Genome Res* **13**, 382–390 (2003).
 59. Li, W. *et al.* Characterization and transplantation of enteric neural crest cells from human induced pluripotent stem cells. *Mol Psychiatry* **23**, 499–508 (2018).
 60. Barber, K., Studer, L. & Fattahi, F. Derivation of enteric neuron lineages from human pluripotent stem cells. *Nat. Protoc.* **14**, 1261–1279 (2019).
 61. Gogolou, A., Frith, T. J. R. & Tsakiridis, A. Generating Enteric nervous system progenitors from human pluripotent stem cells. *Curr. Protoc.* **1**, e137 (2021).
 62. Kampmann, M. CRISPRi and CRISPRa Screens in Mammalian Cells for Precision Biology and Medicine. *ACS Chem Biol* **13**, 406–416 (2018).
 63. Laerum, O. D., Steinsvåg, S. & Bjerkvig, R. Cell and tissue culture of the central nervous system: recent developments and current applications. *Acta Neurol Scand* **72**, 529–549 (1985).
 64. Gurdon, J. B. & Hopwood, N. The introduction of *Xenopus laevis* into developmental biology: of empire, pregnancy testing and ribosomal genes. *Int J Dev Biol* **44**, 43–50 (2000).

65. Harland, R. M. & Grainger, R. M. *Xenopus* research: metamorphosed by genetics and genomics. *Trends Genet* **27**, 507–515 (2011).
66. Hellsten, U. *et al.* The genome of the Western clawed frog *Xenopus tropicalis*. *Science* **328**, 633–636 (2010).
67. Bhattacharya, D., Marfo, C. A., Li, D., Lane, M. & Khokha, M. K. CRISPR/Cas9: An inexpensive, efficient loss of function tool to screen human disease genes in *Xenopus*. *Dev Biol* **408**, 196–204 (2015).
68. Exner, C. R. T. & Willsey, H. R. *Xenopus* leads the way: Frogs as a pioneering model to understand the human brain. *Genesis* **59**, e23405 (2021).
69. Moody, S. A. Fates of the blastomeres of the 16-cell stage *Xenopus* embryo. *Dev Biol* **119**, 560–578 (1987).
70. Moody, S. A. Fates of the blastomeres of the 32-cell-stage *Xenopus* embryo. *Dev Biol* **122**, 300–319 (1987).
71. Willsey, H. R. *et al.* Parallel in vivo analysis of large-effect autism genes implicates cortical neurogenesis and estrogen in risk and resilience. *Neuron* **109**, 788–804.e8 (2021).
72. Willsey, H. R. *et al.* The neurodevelopmental disorder risk gene DYRK1A is required for ciliogenesis and control of brain size in *Xenopus* embryos. *Development* **147**, (2020).
73. DeLay, B. D. *et al.* Tissue-Specific Gene Inactivation in *Xenopus laevis*: Knockout of *lhx1* in the Kidney with CRISPR/Cas9. *Genetics* **208**, 673–686 (2018).
74. Willsey, H. R. *et al.* Modelling human genetic disorders in *Xenopus tropicalis*. *Dis Model Mech* **17**, (2024).

75. Womble, M., Pickett, M. & Nascone-Yoder, N. Frogs as integrative models for understanding digestive organ development and evolution. *Semin Cell Dev Biol* **51**, 92–105 (2016).
76. Chalmers, A. D. & Slack, J. M. Development of the gut in *Xenopus laevis*. *Dev Dyn*. **212**, 509–521 (1998).
77. Epperlein, H. H., Krotoski, D., Halfter, W. & Frey, A. Origin and distribution of enteric neurones in *Xenopus*. *Anat Embryol (Berl)* **182**, 53–67 (1990).
78. Holmberg, A., Hägg, U., Fritsche, R. & Holmgren, S. Occurrence of neurotrophin receptors and transmitters in the developing *Xenopus* gut. *Cell Tissue Res*. **306**, 35–47 (2001).
79. Sundqvist, M. & Holmgren, S. Neurotrophin receptors and enteric neuronal development during metamorphosis in the amphibian *Xenopus laevis*. *Cell Tissue Res*. **316**, 45–54 (2004).
80. Mittal, R. *et al.* Neurotransmitters: The Critical Modulators Regulating Gut-Brain Axis. *J Cell Physiol* **232**, 2359–2372 (2017).
81. Olsson, C. Distribution and effects of PACAP, VIP, nitric oxide and GABA in the gut of the African clawed frog *Xenopus laevis*. *J Exp Biol* **205**, 1123–1134 (2002).
82. Sundqvist, M. & Holmgren, S. Ontogeny of excitatory and inhibitory control of gastrointestinal motility in the African clawed frog, *Xenopus laevis*. *Am J Physiol Regul Integr Comp Physiol* **291**, R1138–44 (2006).
83. Young, H. M., Bergner, A. J. & Müller, T. Acquisition of neuronal and glial markers by neural crest-derived cells in the mouse intestine. *J Comp Neurol* **456**, 1–11 (2003).

84. Elworthy, S., Pinto, J. P., Pettifer, A., Cancela, M. L. & Kelsh, R. N. Phox2b function in the enteric nervous system is conserved in zebrafish and is sox10-dependent. *Mech. Dev.* **122**, 659–669 (2005).
85. Talikka, M., Stefani, G., Brivanlou, A. H. & Zimmerman, K. Characterization of *Xenopus* Phox2a and Phox2b defines expression domains within the embryonic nervous system and early heart field. *Gene Expr Patterns* **4**, 601–607 (2004).
86. Owens, N. D. L. *et al.* Measuring Absolute RNA Copy Numbers at High Temporal Resolution Reveals Transcriptome Kinetics in Development. *Cell Rep* **14**, 632–647 (2016).
87. Fisher, M. *et al.* Xenbase: key features and resources of the *Xenopus* model organism knowledgebase. *Genetics* **224**, (2023).
88. Pattyn, A., Morin, X., Cremer, H., Golidis, C. & Brunet, J. F. Expression and interactions of the two closely related homeobox genes Phox2a and Phox2b during neurogenesis. *Development* **124**, 4065–4075 (1997).
89. Perrone-Bizzozero, N. & Bolognani, F. Role of HuD and other RNA-binding proteins in neural development and plasticity. *J Neurosci Res* **68**, 121–126 (2002).
90. Sanders, K. M. & Ward, S. M. Nitric oxide and its role as a non-adrenergic, non-cholinergic inhibitory neurotransmitter in the gastrointestinal tract. *Br J Pharmacol* **176**, 212–227 (2019).
91. Taraviras, S. *et al.* Signalling by the RET receptor tyrosine kinase and its role in the development of the mammalian enteric nervous system. *Development* **126**, 2785–2797 (1999).
92. Natarajan, D., McCann, C., Dattani, J., Pachnis, V. & Thapar, N. Multiple Roles of

- Ret Signalling During Enteric Neurogenesis. *Front Mol Neurosci* **15**, 832317 (2022).
93. Carlomagno, F. *et al.* The kinase inhibitor PP1 blocks tumorigenesis induced by RET oncogenes. *Cancer Res* **62**, 1077–1082 (2002).
 94. Knowles, P. P. *et al.* Structure and chemical inhibition of the RET tyrosine kinase domain. *J Biol Chem* **281**, 33577–33587 (2006).
 95. Traeger, L., Kroon, H. M., Bedrikovetski, S., Moore, J. W. & Sammour, T. The impact of acetylcholinesterase inhibitors on ileus and gut motility following abdominal surgery: a clinical review. *ANZ J Surg* **92**, 69–76 (2022).
 96. Broadley, K. J. & Kelly, D. R. Muscarinic receptor agonists and antagonists. *Molecules* **6**, 142–193 (2001).
 97. Saffran, M., Pansky, B., Budd, G. C. & Williams, F. E. Insulin and the gastrointestinal tract. *J. Control. Release* **46**, 89–98 (1997).
 98. Rtibi, K. *et al.* Vinblastine, an anticancer drug, causes constipation and oxidative stress as well as others disruptions in intestinal tract in rat. *Toxicol Rep* **4**, 221–225 (2017).
 99. Sikander, A., Rana, S. V. & Prasad, K. K. Role of serotonin in gastrointestinal motility and irritable bowel syndrome. *Clin. Chim. Acta* **403**, 47–55 (2009).
 100. Dershowitz, L. B., Li, L., Pasca, A. M. & Kaltschmidt, J. A. Anatomical and functional maturation of the mid-gestation human enteric nervous system. *Nat Commun* **14**, 2680 (2023).
 101. Pearl, E. J., Grainger, R. M., Guille, M. & Horb, M. E. Development of Xenopus resource centers: the National Xenopus Resource and the European Xenopus Resource Center. *Genesis* **50**, 155–163 (2012).

102. Sive, H. L., Grainger, R. M. & Harland, R. M. *Early Development of Xenopus Laevis: A Laboratory Manual*. (CSHL Press, 2000).
103. Willsey, H. R. Whole-Mount RNA In Situ Hybridization and Immunofluorescence of Xenopus Embryos and Tadpoles. *Cold Spring Harb. Protoc.* **2021**, db.prot105635 (2021).
104. Sive, H. L., Grainger, R. M. & Harland, R. M. Baskets for in situ hybridization and immunohistochemistry. *CSH Protoc.* **2007**, db.prot4777 (2007).
105. Li, M. *et al.* Integrative functional genomic analysis of human brain development and neuropsychiatric risks. *Science* **362**, (2018).
106. Polioudakis, D. *et al.* A Single-Cell Transcriptomic Atlas of Human Neocortical Development during Mid-gestation. *Neuron* **103**, 785–801.e8 (2019).
107. Fan, X. *et al.* Spatial transcriptomic survey of human embryonic cerebral cortex by single-cell RNA-seq analysis. *Cell Res.* **28**, 730–745 (2018).
108. Willsey, A. J. *et al.* Coexpression networks implicate human midfetal deep cortical projection neurons in the pathogenesis of autism. *Cell* **155**, 997–1007 (2013).
109. Weinschutz Mendes, H. *et al.* High-throughput functional analysis of autism genes in zebrafish identifies convergence in dopaminergic and neuroimmune pathways. *Cell Rep.* **42**, 112243 (2023).
110. Birtele, M. *et al.* Non-synaptic function of the autism spectrum disorder-associated gene SYNGAP1 in cortical neurogenesis. *Nat. Neurosci.* **26**, 2090–2103 (2023).
111. Nagy, N. & Goldstein, A. M. Enteric nervous system development: A crest cell's journey from neural tube to colon. *Semin. Cell Dev. Biol.* **66**, 94–106 (2017).
112. Sestan, N. & State, M. W. Lost in Translation: Traversing the Complex Path from

- Genomics to Therapeutics in Autism Spectrum Disorder. *Neuron* **100**, 406–423 (2018).
113. Willsey, A. J. *et al.* The Psychiatric Cell Map Initiative: A Convergent Systems Biological Approach to Illuminating Key Molecular Pathways in Neuropsychiatric Disorders. *Cell* **174**, 505–520 (2018).
114. Nakayama, T. *et al.* Cas9-based genome editing in *Xenopus tropicalis*. *Methods Enzymol.* **546**, 355–375 (2014).
115. Willsey, H. R. *et al.* Katanin-like protein *Katnal2* is required for ciliogenesis and brain development in *Xenopus* embryos. *Dev. Biol.* **442**, 276–287 (2018).
116. Holloway, E. M. *et al.* Mapping Development of the Human Intestinal Niche at Single-Cell Resolution. *Cell Stem Cell* **28**, 568–580.e4 (2021).
117. Simons Vip Consortium. Simons Variation in Individuals Project (Simons VIP): a genetics-first approach to studying autism spectrum and related neurodevelopmental disorders. *Neuron* **73**, 1063–1067 (2012).
118. Furness, J. B. The enteric nervous system and neurogastroenterology. *Nat. Rev. Gastroenterol. Hepatol.* **9**, 286–294 (2012).
119. Blackburn, A. T. M. *et al.* *DYRK1A*-related intellectual disability: a syndrome associated with congenital anomalies of the kidney and urinary tract. *Genet. Med.* **21**, 2755–2764 (2019).
120. Johnson, H. K., Wahl, S. E., Sesay, F., Litovchik, L. & Dickinson, A. J. G. *Dyrk1a* is required for craniofacial development in *Xenopus laevis*. *Developmental Biology* **511**, 63–75 (2024).
121. Tobin, J. L. *et al.* Inhibition of neural crest migration underlies craniofacial

- dysmorphology and Hirschsprung's disease in Bardet-Biedl syndrome. *Proc. Natl. Acad. Sci. U. S. A.* **105**, 6714–6719 (2008).
122. Honoré, S. M., Aybar, M. J. & Mayor, R. Sox10 is required for the early development of the prospective neural crest in *Xenopus* embryos. *Dev. Biol.* **260**, 79–96 (2003).
123. Alkobtawi, M. *et al.* Characterization of Pax3 and Sox10 transgenic *Xenopus laevis* embryos as tools to study neural crest development. *Dev. Biol.* **444 Suppl 1**, S202–S208 (2018).
124. Göckler, N. *et al.* Harmine specifically inhibits protein kinase DYRK1A and interferes with neurite formation. *FEBS J.* **276**, 6324–6337 (2009).
125. Ederly, P. *et al.* Mutations of the RET proto-oncogene in Hirschsprung's disease. *Nature* **367**, 378–380 (1994).
126. Tomuschat, C. & Puri, P. RET gene is a major risk factor for Hirschsprung's disease: a meta-analysis. *Pediatr. Surg. Int.* **31**, 701–710 (2015).
127. Lieberman. *Monoamine Oxidase Inhibitors in Neurological Diseases*. (CRC Press, 1994).
128. Jin, J. G., Foxx-Orenstein, A. E. & Grider, J. R. Propulsion in guinea pig colon induced by 5-hydroxytryptamine (HT) via 5-HT₄ and 5-HT₃ receptors. *J. Pharmacol. Exp. Ther.* **288**, 93–97 (1999).
129. Haga, K., Asano, K., Fukuda, T. & Kobayakawa, T. The function of 5-HT₃ receptors on colonic transit in rats. *Obes. Res.* **3 Suppl 5**, 801S–810S (1995).
130. Chen, J. J. *et al.* Maintenance of serotonin in the intestinal mucosa and ganglia of mice that lack the high-affinity serotonin transporter: Abnormal intestinal motility

- and the expression of cation transporters. *J. Neurosci.* **21**, 6348–6361 (2001).
131. Grider, J. R., Kuemmerle, J. F. & Jin, J. G. 5-HT released by mucosal stimuli initiates peristalsis by activating 5-HT₄/5-HT_{1p} receptors on sensory CGRP neurons. *Am. J. Physiol.* **270**, G778–82 (1996).
132. Schechter, L. E. *et al.* Neuropharmacological profile of novel and selective 5-HT₆ receptor agonists: WAY-181187 and WAY-208466. *Neuropsychopharmacology* **33**, 1323–1335 (2008).
133. Localization of 5-HT₆ receptors at the plasma membrane of neuronal cilia in the rat brain. *Brain Res.* **872**, 271–275 (2000).
134. Rao, M. & Gershon, M. D. The bowel and beyond: the enteric nervous system in neurological disorders. *Nat. Rev. Gastroenterol. Hepatol.* (2016).
135. Rolic, A. S. *et al.* The enteric nervous system promotes intestinal health by constraining microbiota composition. *PLoS Biol.* **15**, e2000689 (2017).
136. Meng, X. *et al.* Assembloid CRISPR screens reveal impact of disease genes in human neurodevelopment. *Nature* **622**, 359–366 (2023).
137. Loukil, A. *et al.* Identification of new ciliary signaling pathways in the brain and insights into neurological disorders. *bioRxiv* (2023) doi:10.1101/2023.12.20.572700.
138. Zahn, N. *et al.* Normal Table of *Xenopus* development: a new graphical resource. *Development* **149**, (2022).
139. Elmentaite, R. *et al.* Single-Cell Sequencing of Developing Human Gut Reveals Transcriptional Links to Childhood Crohn's Disease. *Dev. Cell* **55**, 771–783.e5 (2020).
140. Lasser, M. *et al.* Pleiotropy of autism-associated chromatin regulators.

Development **150**, (2023).

141. Lingeman, E., Jeans, C. & Corn, J. E. Production of Purified CasRNPs for Efficacious Genome Editing. *Curr. Protoc. Mol. Biol.* **120**, 31.10.1–31.10.19 (2017).
142. Choi, H. M. T. *et al.* Third-generation in situ hybridization chain reaction: multiplexed, quantitative, sensitive, versatile, robust. *Development* **145**, (2018).

Publishing Agreement

It is the policy of the University to encourage open access and broad distribution of all theses, dissertations, and manuscripts. The Graduate Division will facilitate the distribution of UCSF theses, dissertations, and manuscripts to the UCSF Library for open access and distribution. UCSF will make such theses, dissertations, and manuscripts accessible to the public and will take reasonable steps to preserve these works in perpetuity.

I hereby grant the non-exclusive, perpetual right to The Regents of the University of California to reproduce, publicly display, distribute, preserve, and publish copies of my thesis, dissertation, or manuscript in any form or media, now existing or later derived, including access online for teaching, research, and public service purposes.

Signed by:

Kate Elizabeth McCluskey

0445B01C0D6E48D...

Author Signature

12/12/2024

Date